CLASSIFICATION OF 2-BRIDGE KNOTS

by

Doğancan Karabaş

B.S, in Mathematics, Boğaziçi University, 2014

B.S, in Physics, Boğaziçi University, 2014

Submitted to the Institute for Graduate Studies in
Science and Engineering in partial fulfillment of
the requirements for the degree of
Master of Science

Graduate Program in Mathematics
Boğaziçi University
2016

CLASSIFICATION OF 2-BRIDGE KNOTS

APPROVED BY:

Assist. Prof. Çağrı Karakurt .....
(Thesis Supervisor)

Prof. Tolga Etgü .....

Assoc. Prof. Burak Gürel .....

DATE OF APPROVAL: 18.01.2016

ACKNOWLEDGEMENTS

I am indebted to my thesis supervisor Çağrı Karakurt. This thesis would not have been possible without his help and support. I also thank TÜBITAK for its financial support.

ABSTRACT

CLASSIFICATION OF 2-BRIDGE KNOTS

In this thesis, we classify the 2-bridge knots, the nontrivial knots which have a knot diagram with two local maxima and minima. They are in some sense the simplest type of knots after the trivial knot. To understand these knots, we focus on a particular representation of them, the Schubert normal form, which generates all the information about the structure of these knots, taking only two integers as an input. To complete the classification, we exploit the connection between knots and 3-manifolds. We show that Lens spaces are the double branched coverings of the 3-dimensional sphere branched along 2-bridge knots, hence we get the classification of 2-bridge knots using the classification of Lens spaces.

ÖZET

2-KÖPRÜLÜ DÜĞÜMLERİN SINIFLANDIRILMASI

Bu tezde iki lokal maksimum ve minimumlu düğüm diyagramı olan, bariz olmayan düğümleri, yani 2-köprülü düğümleri sınıflandırıyoruz. Bunlar bir bakıma bariz düğümden sonraki en basit yapıdaki düğüm olma özelliğini taşıyor. Bu düğümleri anlamak için onların Schubert normal formu adındaki, sadece iki tam sayı alarak onların tüm yapısı hakkında bilgi veren özel bir reprezantasyonuna odaklanıyoruz. Sınıflandırmayı tamamlamak için, düğümler ve üç boyutlu çokkatlılar arasındaki bağlantıyı kullanıyoruz. Lens uzaylarının üç boyutlu kürenin 2-köprülü düğümler üzerinden dallanmış çift örtüsü olduğunu gösteriyoruz, böylece Lens uzaylarının sınıflandırılmasını kullanarak 2 köprülü düğümlerin sınıflandırılmasını elde ediyoruz.

TABLE OF CONTENTS

ACKNOWLEDGEMENTS iii
ABSTRACT iv
ÖZET v
LIST OF FIGURES vii
LIST OF SYMBOLS x
1. INTRODUCTION xi
2. BACKGROUND 1
3. CLASSIFICATION OF 2-BRIDGE KNOTS 14
3.1. Schubert Normal Form 14
3.2. Heegaard Diagrams 25
3.3. Branched Coverings 33
3.4. Classification of 2-Bridge Knots 37
4. CONCLUSION 43
REFERENCES 44

LIST OF FIGURES

Figure 2.1. Right-handed trefoil. 2

Figure 2.2. The knot diagram d in E-plane. 4

Figure 2.3. Two arcs bound a simply connected region inside. 7

Figure 2.4. Two arcs bound a simply connected region outside. 8

Figure 2.5. Bridges of the right-handed trefoil. 9

Figure 2.6. A 3-bridge representation of the right-handed trefoil. 9

Figure 2.7. Right-handed trefoil with two local maxima and minima. 10

Figure 2.8. Transforming right handed trefoil to its 2-bridge representation (Step 1). 11

Figure 2.9. Transforming right handed trefoil to its 2-bridge representation (Step 2). 11

Figure 2.10. Transforming right handed trefoil to its 2-bridge representation (Step 3). 12

Figure 2.11. Transforming right handed trefoil to its 2-bridge representation (Step 4). 12

Figure 2.12. A 2-bridge representation of the right-handed trefoil. 13

Figure 3.1. A 2-bridge representation of the right-handed trefoil with the intersection points on α-arcs labelled. 16

Figure 3.2. The two arcs γ and γ' connecting $\beta_j(n)$ and $\beta_j(n+1)$. 18

Figure 3.3. $\alpha_{i_1} \setminus \{\beta_j(n)\}$ lies inside of $\gamma \cup \gamma'$. 19

Figure 3.4. $\alpha_{i_1} \setminus \{\beta_j(n)\}$ lies outside of $\gamma \cup \gamma'$. 19

Figure 3.5. α_i with double labelled crossing points. 20

Figure 3.6. β_1 with its initial conditions. 21

Figure 3.7. β_1 when α-arcs considered as circles. 22

Figure 3.8. The 2-bridge knot with $p = 3$ and $q = 1$ (α-arcs considered as circles). 24

Figure 3.9. $S(5, 3)$ (The figure-eight knot). 24

Figure 3.10. Genus g handlebody (with solid interior). 25

Figure 3.11. Genus 0 Heegaard decomposition of S^3 (considered as $D^3/\partial D^3$). . 26

Figure 3.12. Genus 1 Heegaard decomposition of S^3 (considered as $D^3/\partial D^3$). . 27

Figure 3.13. A Heegaard diagram $(\Sigma_1, \alpha_1, \beta_1)$ of S^3. 28

Figure 3.14. A Heegaard diagram $(\Sigma_1, \alpha_1, \beta_1)$ of $S^1 \times S^2$. 29

Figure 3.15. A genus 2 Heegaard diagram. 31

Figure 3.16. Meridians and longitudes of Σ_g. 31

Figure 3.17. The double branched covering of D^2 branched along one point. . . 34

Figure 3.18. The double branched covering of S^2 branched along $2g+2$ points. 35

Figure 3.19. The double branched covering of D^3 branched along $g+1$ arcs. . . 36

Figure 3.20. $S(3,1)$ in S^3. 37

Figure 3.21. The lifts of the arcs $\alpha_1, \alpha_2, \gamma_1, \gamma_2$. 39

Figure 3.22. Intersections between β_1 and γ_1. 40

LIST OF SYMBOLS

D^n	Closed n-dimensional disk
$\operatorname{Int} A$	Interior of the set A
S^n	n-dimensional sphere
$\operatorname{sign} m$	Sign of the integer m

1. INTRODUCTION

Our aim is to classify 2-bridge knots. This is done first by Schubert in [1]. His techniques involve geometric analysis of the problem. But we will follow the strategy used in [2]. First, we will prove Corollary 3.8, which shows that all 2-bridge knots can be represented by a Schubert normal form $S(p, q)$. Then, we will prove Theorem 3.17, which classify all Schubert normal forms, hence 2-bridge knots, using the classification of Lens space and the fact that the double branched coverings of S^3 branched along $S(p, q)$ is the Lens space $L(p, q)$. Although the general strategy is the same with [2], our proofs are different from [2].

2. BACKGROUND

We will begin with the background material related to knots and in particular, n-bridge representations.

A *knot* k is a (topological) embedding of S^1 into $\mathbb{R}^3$, or S^3. The image of this map, $k\left(S^1\right)$, is also considered as the knot. In this thesis, all maps are also used to represent their image, it depends on the context. For example, we will write k instead of $k\left(S^1\right)$ when we talk about the image of the knot.

Two embeddings, $f_0, f_1 : X \to Y$ are *isotopic* if there is an embedding,

$$F : X \times I \to Y \times I$$

such that $F(x,t) = (f(x,t),t)$ for some $f : X \times I \to Y$, with $f(x,0) = f_0(x)$ and $f(x,1) = f_1(x)$. F is called a *level-preserving isotopy* connecting f_0 and f_1. We use the notation $f_t(x) = f(x,t)$.

Two embeddings, $f_0, f_1 : X \to Y$ are *ambient isotopic* if there is a level-preserving isotopy

$$H : Y \times I \to Y \times I$$

such that $H(y,t) = (h_t(y),t)$, with $h_0 = id_Y$ and $f_1 = h_1 f_0$. H is called an *ambient isotopy.*

Two knots are *equivalent* if they are ambient isotopic. Equivalence class of a knot k is denoted by $[k]$.

A knot is *tame* if it is equivalent to a simple closed polygon in $\mathbb{R}^3$. A knot is *wild* if it is not tame. From now on, all knots are assumed to be tame.

A projection of a knot k into a plane E (isomorphic to $\mathbb{R}^2$, but considered as S^2) in $\mathbb{R}^3$ is a *knot diagram* of k if it has finitely many multiple points (points in E whose preimage contains more than one point), all multiple points are double points (points in E whose preimage contains exactly two points) and at each double point, arcs of the diagram intersect transversally. A double point in a knot diagram is called a *crossing* and crossings are marked so that a knot can be reconstructed from its knot diagram. We usually consider a crossing as two separate points, and call them as an *overcrossing* and an *undercrossing* according to their positions on the knot. For a given knot k, the set of all knot diagrams of all knots in the equivalence class of k is denoted by $D[k]$.

For example, a knot diagram of the knot right-handed trefoil can be seen in Figure 2.1.

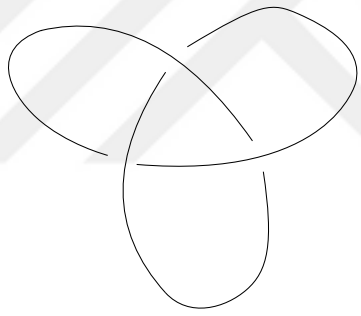

Figure 2.1. Right-handed trefoil.

Two knot diagrams are *equal* if they are isotopic in E (considered as S^2) as graphs, where the isotopy respects overcrossings and undercrossings. Two knot diagrams are *equivalent* if they can be connected by a finite sequence of Reidemeister moves. For the definition of the Reidemeister moves, see [2]. We also know that two knots are equivalent if and only if all their diagrams are equivalent.

For a knot $k : S^1 \to \mathbb{R}^3$, the *bridge number* of k is defined as

$$b(k) := \min_{l \in [k]} \{M(\pi_z l)\}$$

where $\pi_z : \mathbb{R}^3 \to \mathbb{R}$ is the projection onto z-axis and $M(\pi_z l)$ is the number of local maxima of the map $\pi_z l$. We could also define the bridge number of k as

$$b(k) := \min_{l \in [k]} \{m(\pi_z l)\}$$

where $m(\pi_z l)$ is the number of local minima of the map $\pi_z l$, since $M(\pi_z l) = m(\pi_z l)$. That is because l is the an embedding of S^1 and as a result, $\pi_z l$ attains its local maxima and minima alternately. Obviously, bridge number is an invariant for knots and it is at least 1.

Also, we say that k is an *n-bridge knot* if $b(k) = n$.

Proposition 2.1. *For any knot k,*

$$b(k) = \min_{d \in D[k], v \in E} \{M(\pi_v d)\} = \min_{d \in D[k], v \in E} \{m(\pi_v d)\}$$

where E is the codomain of d.

Proof. Define $c(k) := \min_{d \in D[k], v \in \mathbb{R}^2} \{M(\pi_v d)\}$. Pick an arbitrary $l \in [k]$. Define E as the yz-plane in $\mathbb{R}^3$ and $d := pl$ where $p : \mathbb{R}^3 \to E$ is the projection onto E. Then d is a knot diagram of l, i.e. $d \in D[k]$ (if it doesn't satisfy the requirements to be a knot diagram, just change l by an ambient isotopy so that d becomes a knot diagram). In this case, we have $\pi_z l = \pi_z d$, in particular $M(\pi_z l) = M(\pi_z d)$. Then $M(\pi_z l) \geq c(k)$. l was arbitrary, hence $b(k) \geq c(k)$.

For the converse, pick an arbitrary $d \in D[k]$ and $v \in E$. Then $d : S^1 \to \mathbb{R}^3 \to E$ is a knot diagram of l' for some $l' \in [k]$. By translating and rotating l' (which are ambient isotopies), we can get an equivalent knot l for which the plane E becomes yz-plane and the vector v becomes z-vector. This gives $\pi_v d = \pi_z l$, in particular $M(\pi_v d) = M(\pi_z l)$. Then $M(\pi_v d) \geq b(k)$. $d \in D[k]$ and $v \in E$ were arbitrary, hence $c(k) \geq b(k)$.

Therefore $b(k) = c(k) = \min_{d \in D[k], v \in E} \{M(\pi_v d)\}$. $b(k) = \min_{d \in D[k], v \in E} \{m(\pi_v d)\}$

can be proved similarly. □

Proposition 2.2. *A knot k is the unknot if and only if $b(k) = 1$.*

Proof. If k is the unknot, then there is $l \in [k]$ such that the image of l is a circle in yz-plane. Hence $M(\pi_z l) = 1$ which gives $b(k) \leq 1$. But in general, we have $b(k) \geq 1$. Therefore, $b(k) = 1$.

Conversely, if $b(k) = 1$, then by Proposition 2.1, there exist $d \in D[k]$ and $v \in E$ (E is the codomain of d) such that $\pi_v d$ has exactly one maximum and one minimum. If we remove this maximum and minimum from the diagram d, we get two curves in E such that their projections into v-axis are injective, since they no local maximum and minimum. This implies that the images of crossing points under the map π_v have all different values. Then d looks as in Figure 2.2. By starting from the crossing with the highest v-coordinate, and proceeding with crossings with lower v-coordinates, we can get rid of every crossing inductively, using Reidemeister moves. By definition, d has only finitely many crossings, so we need only finitely many Reidemeister moves to get rid of all crossings. This implies that d is equivalent to a diagram which has no crossing. Hence knots that they represent must be equivalent also, i.e. k and unknot must be equivalent. Therefore, k is the unknot.

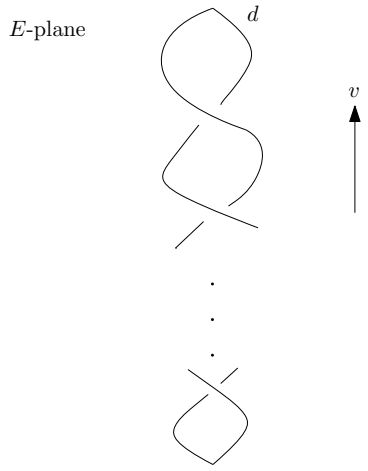

Figure 2.2. The knot diagram d in E-plane.

□

For any knot diagram d, a curve (including its endpoints) on d is an *overbridge* of d if it has at least one overcrossing, has zero undercrossing and it is maximal, i.e. there is no curve with more overcrossings and zero undercrossing which contains it. A curve (including its endpoints) is an *underbridge* of d if it has at least one undercrossing, has zero overcrossing and it is maximal, i.e. there is no curve with more undercrossings and zero overcrossing which contains it. Denote the number of overbridges of d by $o(d)$ and the number of underbridges of d by $u(d)$.

Proposition 2.3. *For any knot k with $b(k) > 1$,*

$$b(k) = \min_{d \in D[k]} \{o(d)\} = \min_{d \in D[k]} \{u(d)\}$$

and for any knot k with $b(k) = 1$,

$$0 = \min_{d \in D[k]} \{o(d)\} = \min_{d \in D[k]} \{u(d)\}.$$

Proof. Assume $b(k) > 1$. Then by Proposition 2.2, k is not an unknot. Therefore every $d \in D[k]$ has at least one crossing, so there are overbridges and underbridges in d. Obviously, d can be written as the union of its overbridges and underbridges. Since d has finitely many crossings, there are finitely many bridges in d. Also by definition, bridges are maximal, so overbridges are connected to underbridges and underbridges are connected to overbridges. S^1 is the domain of d, so $o(d) = u(d)$.

Pick a vector w in $\mathbb{R}^3$ such that w is perpendicular to E (E is the codomain of d) and the direction w respects overcrossings and undercrossings of d. If we pull overbridges along positive w-direction and underbridges along negative w-direction, we construct an equivalent knot l' which has d as a knot diagram and $\pi_w l'$ has $o(d)$ maxima and $u(d)$ minima. By rotating l', we can get an equivalent knot l such that the w-vector becomes z-vector and $\pi_z l$ has $o(d)$ maxima and $u(d)$ minima. This implies $o(d) \geq b(k) = \min_{l \in [k]} \{M(\pi_z l)\} = b(k)$, hence $\min_{d \in D[k]} \{o(d)\} \geq b(k)$.

Conversely, if $l \in [k]$ and if we define E as xy-plane, then for a knot diagram d

of l which has E as its codomain, obviously we have $M(\pi_z l) \geq o(d)$. Hence $M(\pi_z l) \geq \min_{d \in D[k]}\{o(d)\}$ and since this is true for all $l \in [k]$, $b(k) \geq \min_{d \in D[k]}\{o(d)\}$.

Combining these results, we get $b(k) = \min_{d \in D[k]}\{o(d)\} = \min_{d \in D[k]}\{u(d)\}$.

Lastly, assume b(k) = 1. By Proposition 2.2, k is the unknot. Then obviously, k has a knot diagram d with no crossing, hence d has no overbridge and underbridge, i.e. $o(d) = u(d) = 0$. Therefore $0 = \min_{d \in D[k]}\{o(d)\} = \min_{d \in D[k]}\{u(d)\}$. $\square$

For a knot diagram d of a nontrivial oriented knot k, define $n := o(d) = u(d)$. Denote the underbridges of d as $\alpha_1, \alpha_2, \ldots, \alpha_n$ and the overbridges of d as $\beta_1, \beta_2, \ldots, \beta_n$ such that they are mutually disjoint except at the crossings and endpoints, and their union is d so that α_i is followed by β_i for $i = 1, 2, \ldots, n$, β_i is followed by α_{i+1} for $i = 1, 2, \ldots, n-1$ and β_n is followed by α_1.

This implies that β_i first intesects with α_i and lastly intersects with α_{i+1} (β_n lastly intersects with α_1) at their common endpoint. Also, α_i first intesects with β_{i-1} (α_1 first intersects with β_n) and lastly intersects with β_i at their common endpoint.

An endpoint of an α- or a β-arc cannot be a crossing in d, otherwise, since endpoints are always shared by an α-arc and a β-arc, this would mean that they contain a crossing of same type. But it cannot be an overcrossing, since α-arcs don't contain any overcrossing, and it cannot be an undercrossing, since β-arcs don't contain any undercrossing.

We also have $\alpha_i \cap \alpha_j = \emptyset$ for any $i \neq j$, since otherwise α_i and α_j intersect at a crossing in d (they don't have any common endpoint). But then, one of these α-arcs must contain an overcrossing, which is impossible since α-arcs are underbridges. Similarly, we have and $\beta_i \cap \beta_j = \emptyset$ for any $i \neq j$.

Let u and v be the coordinate axes of E (the codomain of d) such that $|u \times v| = 1$.

d is an *n-bridge representation* of k if the following properties are also satisfied by d:

(i) All underbridges of d are line segments that lies on the u-axis so that α_{i+1} is on the right side of α_i for $i = 1, 2, \ldots, n-1$.
(ii) Orientations of underbridges are in the direction of positive u-axis.
(iii) If β_i intesects with α_{j_1} and α_{j_2} successively, then $j_1 \neq j_2$.
(iv) If α_i intesects with β_{j_1} and β_{j_2} successively, then $j_1 \neq j_2$.

Proposition 2.4. *If a nontrivial oriented knot k has a knot diagram d, then k has an n-bridge representation for some n that satisfies $b(k) \leq n \leq o(d)$.*

Proof. Denote the underbridges of d as $\alpha_1, \alpha_2, \ldots, \alpha_n$ and the overbridges of d as $\beta_1, \beta_2, \ldots, \beta_n$ such that they are mutually disjoint except at the crossings and end-points, and their union is d so that α_i is followed by β_i for $i = 1, 2, \ldots, n$, β_i is followed by α_{i+1} for $i = 1, 2, \ldots, n-1$ and β_n is followed by α_1.

By an isotopy, we can change d so that all underbridges of d become line segments that lies on u-axis and their orientations are in the direction of positive u-axis. So, (i) and (ii) are satisfied.

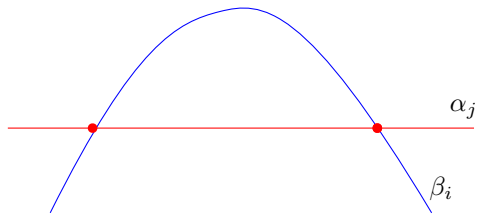

Figure 2.3. Two arcs bound a simply connected region inside.

If β_i intersects with same α_j successively, then we get a simply connected region in E (considered as S^2) that is bounded by the arcs on the curves β_i and α_j (Figure 2.3 and 2.4). By a sequence of Reidemeister moves, we can get rid of these two intersection points. So we can assume that if β_i intersects with α_{j_1} and α_{j_2} successively, then $j_1 \neq j_2$. Hence (iii) is satisfied. Similarly, (iv) is satisfied also.

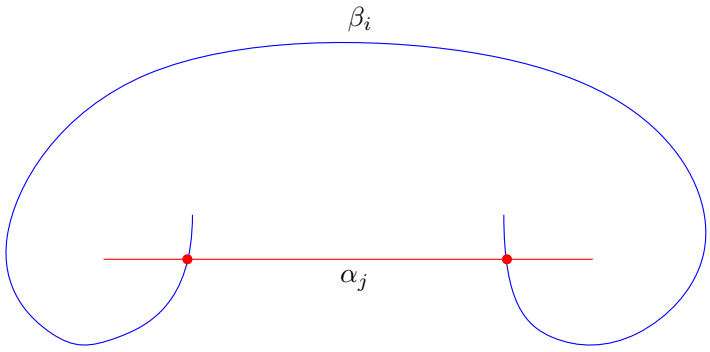

Figure 2.4. Two arcs bound a simply connected region outside.

As a result of Reidemeister moves, we may lose some underbridges and overbridges. Hence, the final diagram will have n overbridges for some $n \leq o(d)$. Also we have $n \geq b(k)$, since otherwise we would get a diagram which have less number of overcrossings than $b(k)$, which contradicts with the minimality of $b(k)$ stated by Proposition 2.3.

Combining these results, we see that k has an n-bridge representation where $b(k) \leq n \leq o(d)$. □

Corollary 2.5. *If k is a nontrivial oriented knot with $n = b(k)$, then k has an n-bridge representation.*

Proof. By Proposition 2.3, $b(k) = \min_{d \in D[k]}\{o(d)\}$. Hence, there exists $d \in D[k]$ with $o(d) = b(k)$. Then by Proposition 2.4, k has an m-bridge representation for some m that satisfies $b(k) \leq m \leq b(k)$, which implies $m = b(k) = n$. Therefore, k has an n-bridge representation. □

As an example, we can consider the right-handed trefoil k with the knot diagram d shown in Figure 2.1. It is easily seen that for this diagram, $o(d) = u(d) = 3$, hence by Proposition 2.4, k has n-bridge representation for some $n \leq 3$. In Figure 2.5, underbridges are shown in red and overbridges are shown in blue. Using isotopy, d becomes 3-bridge represenatation of k as in Figure 2.6.

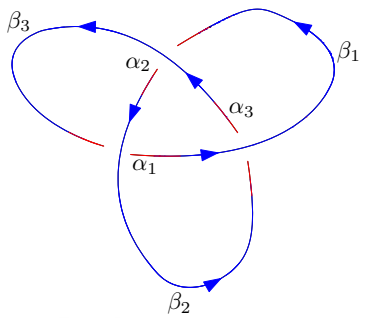

Figure 2.5. Bridges of the right-handed trefoil.

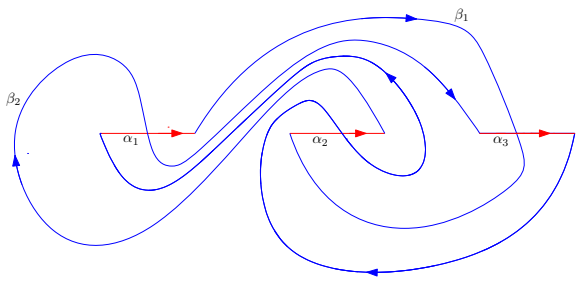

Figure 2.6. A 3-bridge representation of the right-handed trefoil.

But the bridge number of right-handed trefoil is $b(k) = 2$. To see that, note that with respect to y-axis, d has two local maxima (see Figure 2.1). This gives, by Proposition 2.1, that $b(k) \leq 2$. Since k is not unknot, by Proposition 2.2, $b(k) > 1$. Hence, $b(k) = 2$.

By Corollary 2.5, k has a 2-bridge representation. To get that from the Figure 2.1, first pull local maxima along positive y-axis, and local minima along negative y-axis. See Figure 2.7.

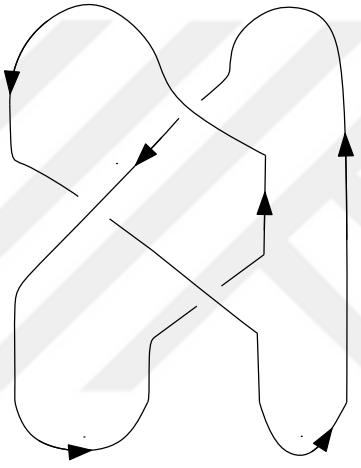

Figure 2.7. Right-handed trefoil with two local maxima and minima.

We want to express d as the union of two overbridges and twp underbridges. See Figure 2.8. We need to transform α-arcs to underbridges and β-arcs to overbridges. To achieve this goal, we must get rid of the intersections of β-arcs with each other by carrying them onto α-arcs. Figure 2.9, 2.10, 2.11 and 2.12 show this process.

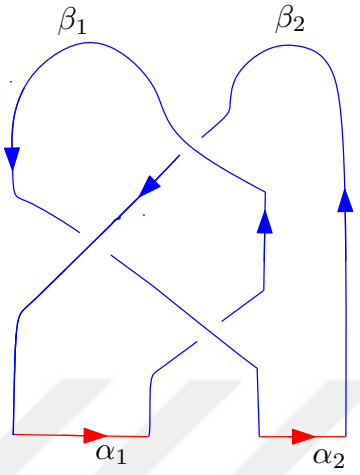

Figure 2.8. Transforming right handed trefoil to its 2-bridge representation (Step 1).

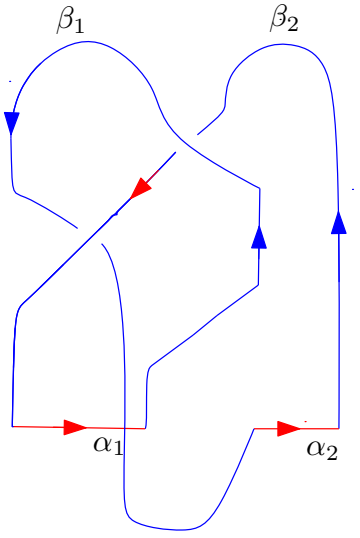

Figure 2.9. Transforming right handed trefoil to its 2-bridge representation (Step 2).

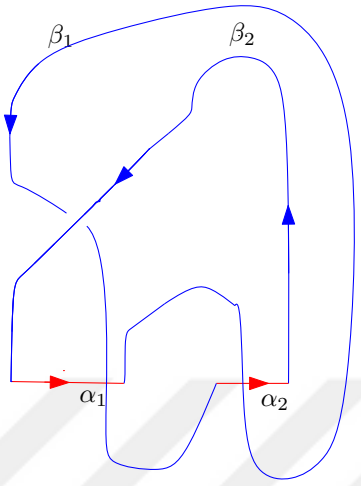

Figure 2.10. Transforming right handed trefoil to its 2-bridge representation (Step 3).

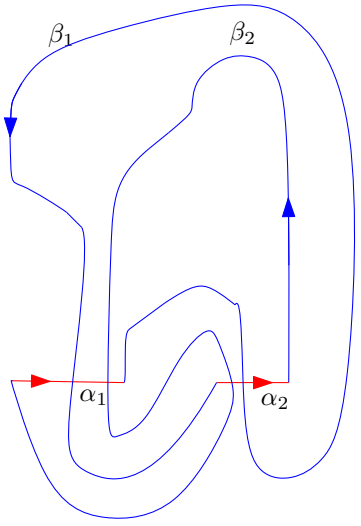

Figure 2.11. Transforming right handed trefoil to its 2-bridge representation (Step 4).

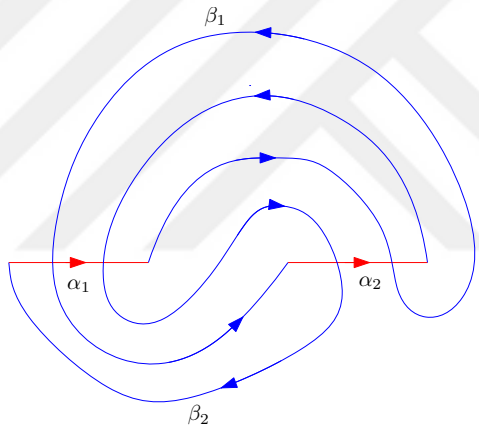

Figure 2.12. A 2-bridge representation of the right-handed trefoil.

3. CLASSIFICATION OF 2-BRIDGE KNOTS

3.1. Schubert Normal Form

We have already known from Corollary 2.5 that every 2-bridge knot has a 2-bridge representation. Now, we want to understand the structure of these representations and at the end of this section we will give them a special name, Schubert normal form.

From now on, for a 2-bridge representation d of a 2-bridge knot k, denote the underbridges of d by α_1, α_2 and the overbridges of d by β_1, β_2 such that they are mutually disjoint except at the crossings and endpoints, and their union is d so that α_1 is followed by β_1, β_1 is followed by α_2, α_2 is followed by β_2 and β_2 is followed by α_1. Let u and v be the coordinate axes of E (the codomain of d) such that $|u \times v| = 1$.

Lemma 3.1. *For a 2-bridge representation d of a 2-bridge knot k, we have*

$$|\alpha_1 \cap \beta_1| = |\alpha_2 \cap \beta_1| = |\alpha_1 \cap \beta_2| = |\alpha_2 \cap \beta_2| \geq 2.$$

Proof. We know that β_1 first intersects with α_1, and by the property (iii) of bridge representations, then intersects with α_2, and it continues intersecting α-arcs alternately. Finally, it intersects with α_2. This implies that $|\alpha_1 \cap \beta_1| = |\alpha_2 \cap \beta_1|$. Similarly, we can show that $|\alpha_1 \cap \beta_1| = |\alpha_1 \cap \beta_2|$ and $|\alpha_1 \cap \beta_2| = |\alpha_2 \cap \beta_2|$.

Furthermore, since α_1 intersects with β_1 at their common endpoint, $|\alpha_1 \cap \beta_1| \geq 1$. In fact, it is greater than 1, since if not, $|\alpha_1 \cap \beta_1| = 1$ and hence $|\alpha_i \cap \beta_j| = 1$ for any $i, j = 1, 2$. This means α- and β-arcs only intersect with each other at their common endpoints, which would mean that d contains no crossings and hence k is an unknot, but k is not an unknot. □

Lemma 3.2. *For a 2-bridge representation d of a 2-bridge knot k, we have*

$$|\alpha_i \cap (\beta_1 \cup \beta_2)| = |\beta_j \cap (\alpha_1 \cup \alpha_2)|$$

for any $i, j = 1, 2$. Furthermore, if we define

$$p := |\alpha_2 \cap (\beta_1 \cup \beta_2)| - 1$$

then p is odd and $p \geq 3$.

Proof. For any $i = 1, 2$, we have

$$\begin{aligned} |\alpha_i \cap (\beta_1 \cup \beta_2)| &= |(\alpha_i \cap \beta_1) \cup (\alpha_i \cap \beta_2)| \\ &= |\alpha_i \cap \beta_1| + |\alpha_i \cap \beta_2| - |\alpha_i \cap \beta_1 \cap \beta_2|. \end{aligned}$$

Now, if $\alpha_i \cap \beta_1 \cap \beta_2$ has an element, it can't be an endpoint of an α- or a β-arc (since endpoints are shared by exactly two curves), hence it must be a crossing in d. But we know from the definition of knot diagrams that all crossings are double points, they cannot be shared by three curves. Therefore $\alpha_i \cap \beta_1 \cap \beta_2 = \emptyset$. So,

$$|\alpha_i \cap (\beta_1 \cup \beta_2)| = |\alpha_i \cap \beta_1| + |\alpha_i \cap \beta_2|$$

for any $i = 1, 2$. Similarly,

$$|\beta_i \cap (\alpha_1 \cup \alpha_2)| = |\beta_i \cap \alpha_1| + |\beta_i \cap \alpha_2|$$

for any $i = 1, 2$. Then, Lemma 3.1 implies

$$|\alpha_i \cap (\beta_1 \cup \beta_2)| = |\beta_i \cap (\alpha_1 \cup \alpha_2)| = 2 \cdot |\alpha_1 \cap \beta_1|$$

for any $i = 1, 2$. Therefore,

$$p = 2 \cdot |\alpha_1 \cap \beta_1| - 1.$$

This implies that p is odd and since $|\alpha_1 \cap \beta_1| \geq 2$ by Lemma 3.1, $p \geq 3$. $\square$

From now on, for a 2-bridge representation d of a 2-bridge knot k, p is defined as in Lemma 3.2 and we will label points of intersections on any α- or β-arc. For any $i, j = 1, 2$ with $i \neq j$, the number of intersection points on α_i is $|\alpha_i \cap (\alpha_j \cup \beta_1 \cup \beta_2)|$ which is equal to $|\alpha_i \cap (\beta_1 \cup \beta_2)|$ since $\alpha_i \cap \alpha_j = \emptyset$. Similarly, for any $i, j = 1, 2$ with $i \neq j$, the number of intersection points on β_i is $|\beta_i \cap (\beta_j \cup \alpha_1 \cup \alpha_2)|$ which is equal to $|\beta_i \cap (\alpha_1 \cup \alpha_2)|$ since $\beta_i \cap \beta_j = \emptyset$. Hence by Lemma 3.2, there are $p+1$ intersection points for any given α- or β-arc. Consider α- and β-arcs as the maps $\alpha_i : [p, 0] \to \mathbb{R}^2$ and $\beta_i : [0, p] \to \mathbb{R}^2$ for $i = 1, 2$. Then, in our convention, $\alpha_i(m)$ and $\beta_i(m)$ will correspond to the intersection points for $m = 0, 1, \ldots, p$. Obviously, $\alpha_i(p)$ and $\alpha_i(0)$ correspond to the endpoints of α_i, and $\beta_i(0)$ and $\beta_i(p)$ correspond to the endpoints of β_i for $i = 1, 2$. The other intersection points correspond to the crossings in d.

Then obviously, $\beta_i(0) = \alpha_i(0)$ for any $i = 1, 2$ and $\beta_i(p) = \alpha_j(p)$ for any $i, j = 1, 2$ with $i \neq j$. We also see that $\alpha_i(m) = \alpha_{i'}(m')$ implies $i = i'$ and $m = m'$, and $\beta_j(n) = \beta_{j'}(n')$ implies $j = j'$ and $n = n'$.

Figure 3.1 shows a 2-bridge representation of the right-handed trefoil (Figure 2.12) with the intersection points on the α-arcs labelled. For this example, $p = 3$. We always label the intersection points according to α-arcs, instead of β-arcs.

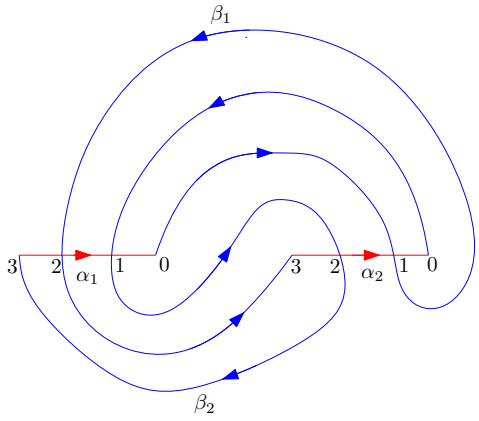

Figure 3.1. A 2-bridge representation of the right-handed trefoil with the intersection points on α-arcs labelled.

Lemma 3.3. *For a 2-bridge representation d of a 2-bridge knot k, $\beta_i(n) = \alpha_j(m)$ implies $n \equiv m \equiv i + j \mod 2$.*

Proof. We know that $\beta_i(0) = \alpha_i(0)$ for any $i = 1, 2$. By the property (iii) of the bridge representations, β_i intersects with α_1 and α_2 alternately. This implies that for any even n, we have $\beta_i(n) = \alpha_i(m)$ and for any odd n, $\beta_i(n) = \alpha_j(m)$ for some m where $i, j = 1, 2$ and $i \neq j$. In any case, $n \equiv i + j \mod 2$. Similarly, we can show $m \equiv i + j \mod 2$. □

Now, define the *algebraic intersection number* of curves γ_1 and γ_2 at their crossing point a as

$$< \gamma_1, \gamma_2 > (a) := \text{sign}|T\gamma_1(a) \times T\gamma_2(a)|$$

where $T\gamma_i(a)$ is the unit tangent vector of γ_i at the point a for $i = 1, 2$. Obviously, the algebraic intersection number of curves at their crossing point can only take the values $1, 0$ or -1 and it is not defined at their endpoints. But note that for an underbridge α and an overbridge β with a as their crossing point, $< \alpha, \beta > (a)$ is either 1 or -1, since α and β intersect transversally by the properties of the knot diagrams. We can define also the *algebraic intersection number* of curves γ_1 and γ_2 as

$$< \gamma_1, \gamma_2 >:= \sum_a < \gamma_1, \gamma_2 > (a)$$

where the sum is taken over all the crossing points a of the curves γ_1 and γ_2.

Lemma 3.4. *Let d and d' be 2-bridge representations which satisfy the following conditions:*

(i) $\alpha_i(m) = \beta_j(n)$ *if and only if* $\alpha'_i(m) = \beta'_j(n)$
(ii) $< \alpha_i, \beta_j > (\alpha_i(m)) =< \alpha'_i, \beta'_j > (\alpha'_i(m))$

for any $i, j = 1, 2$ and $m, n = 1, 2, \ldots, p-1$, where α- and β-arcs are the bridges of d, and α'- and β'-curves are the bridges of d'. Then d and d' are equal as knot diagrams.

Proof. We consider d and d' as knot diagrams in the plane E and want to show that

they are equal. We know that the alignment of α-arcs are exactly given (up to sliding α-arcs along the u-axis) by the properties (i) and (ii) of the bridge representations. Hence, we can assume $\alpha_i = \alpha'_i$ for all i.

In this case, $\alpha_i(m) = \alpha'_i(m)$ for all i and m, therefore by the hypothesis (i), we have $\beta_j(n) = \beta'_j(n)$ for all j and n. Also, we get by using hypothesis (ii) that $< \alpha_i, \beta_j > (\alpha_i(m)) =< \alpha_i, \beta'_j > (\alpha_i(m))$ for all i, j and m. These results imply that β_j and β'_j are totally the same at the intersection points for any j.

It remains to show that the arcs of β_j and β'_j connecting the intersection points are isotopic in E (considered as S^2). For a fixed $j = 1, 2$ and $n = 0, 1, \ldots, p-1$, consider two arcs γ and γ' of β_j and β'_j, respectively, that connect the intersection points $\beta_j(n)$ and $\beta_j(n+1)$.

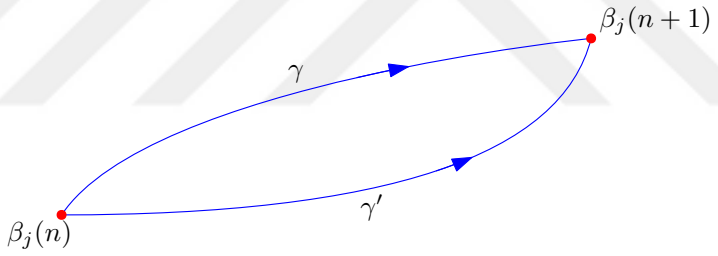

Figure 3.2. The two arcs γ and γ' connecting $\beta_j(n)$ and $\beta_j(n+1)$.

Without losing too much generality, we can assume that these two arcs don't intersect apart from their common endpoints, $n \neq 0$, $p-1$ and $d \setminus \gamma = d' \setminus \gamma'$. Then $\gamma \cup \gamma'$ is a simple closed curve (Figure 3.2). Assume that β_j intersects with α_{i_1} at $\beta_j(n)$ and with α_{i_2} at $\beta_j(n+1)$. Then obviously, $i_1 \neq i_2$. Now, observe that

$$d \setminus \gamma = (\alpha_{i_1} \setminus \{\beta_j(n)\}) \cup (\alpha_{i_2} \setminus \{\beta_j(n+1)\}) \cup (\beta_j \setminus \gamma) \cup \beta_l$$

where $l \neq j$. By hypothesis (ii), we have $< \alpha_{i_1}, \beta_j > (\beta_j(n)) =< \alpha_{i_1}, \beta'_j > (\beta_j(n))$ and hence $\alpha_{i_1} \setminus \{\beta_j(n)\}$ lies either inside of $\gamma \cup \gamma'$ (Figure 3.3) or outside of $\gamma \cup \gamma'$ (Figure 3.4). Similarly, $\alpha_{i_2} \setminus \{\beta_j(n+1)\}$ lies either inside or outside of $\gamma \cup \gamma'$.

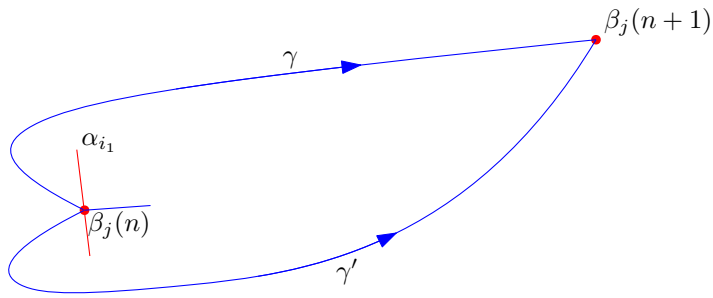

Figure 3.3. $\alpha_{i_1} \setminus \{\beta_j(n)\}$ lies inside of $\gamma \cup \gamma'$.

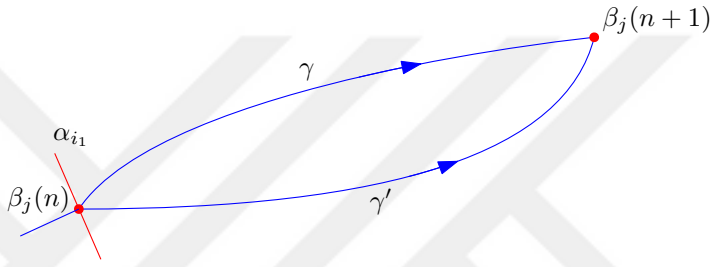

Figure 3.4. $\alpha_{i_1} \setminus \{\beta_j(n)\}$ lies outside of $\gamma \cup \gamma'$.

$\beta_j \setminus \gamma$ and β_l are connected and they don't intersect with $\gamma \cup \gamma'$, so they lie either inside or outside of $\gamma \cup \gamma'$. All α- and β-arcs are connected through their endpoints, hence $\alpha_{i_1} \setminus \{\beta_j(n)\}$, $\alpha_{i_2} \setminus \{\beta_j(n+1)\}$, $\beta_j \setminus \gamma$ and β_l all lie either inside or outside of $\gamma \cup \gamma'$ together. Hence $d \setminus \gamma$ must either lie inside of $\gamma \cup \gamma'$, in which case $\gamma \cup \gamma'$ bounds a simply connected region inside; or outside of $\gamma \cup \gamma'$, in which case, $\gamma \cup \gamma'$ bounds a simply connected region outside, since we consider E as S^2. Hence in any case, γ and γ' are isotopic in E. Also $d \setminus \gamma = d' \setminus \gamma'$, so d and d' are isotopic in E which means by definition that d and d' are equal as knot diagrams. $\square$

Let us define a useful notation which encompasses all the information related to the intersection points. For $i, j = 1, 2$ and $m, n = 1, 2, \ldots, p-1$, if $\beta_j(n) = \alpha_i(m)$ and $< \alpha_i, \beta_j > (\beta_j(n)) = 1$, then we say $\beta_j(n) = \alpha_i[m]$. If $\beta_j(n) = \alpha_i(m)$ and $< \alpha_i, \beta_j > (\beta_j(n)) = -1$, then we say $\beta_j(n) = \alpha_i[2p - m]$. For the endpoints, i.e. for $m, n = 0, p$, if $\beta_j(n) = \alpha_i(m)$, we say $\beta_j(n) = \alpha_i[m]$.

So, for $i, j = 1, 2$, $n = 0, 1, \ldots, p$ and $l = 0, 1, \ldots, 2p-1$, $\beta_j(n) = \alpha_i[l]$ gives all information related to the intersection points, since it gives

(i) $\beta_j(n) = \alpha_i(|m|)$
(ii) $< \alpha_i, \beta_j > (\beta_j(n)) = \text{sign}(m)$

where $m \equiv l \mod 2p$ and $-p < m \leq p$. (ii) is only given if $n \neq 0, p$.

This motivates us to label the right and left side of the crossing points on α-arcs separately. For a crossing point $\alpha_i(m)$, we have $\beta_j(n) = \alpha_i[m]$ if β_j hits α_i from the right and $\beta_j(n) = \alpha_i[2p-m]$ if β_j hits α_i from the left. Then label the right side of $\alpha_i(m)$ as m, the left side of $\alpha_i(m)$ as $2p-m$. See Figure 3.5.

Figure 3.5. α_i with double labelled crossing points.

We can obviously restate Lemma 3.3 and 3.4 in this new notation:

Lemma 3.5. *For a 2-bridge representation d of a 2-bridge knot k, $\beta_i(n) = \alpha_j[m]$ implies $n \equiv m \equiv i + j \mod 2$.*

Lemma 3.6. *Let d and d' be 2-bridge representations which satisfy the condition*

$$\beta_j(n) = \alpha_i[l] \Longleftrightarrow \beta'_j(n) = \alpha'_i[l]$$

for any $i, j = 1, 2$, $n = 0, 1, \ldots, p$ and $l = 0, 1, \ldots, 2p-1$, where α- and β-arcs are the bridges of d, and α'- and β'-curves are the bridges of d'. Then d and d' are equal as knot diagrams.

Theorem 3.7. *Given odd integers p, q with $p \geq 3$, $-p < q < p$ and $\gcd(p, q) = 1$, there is a unique 2-bridge representation satisfying*

(i) $|\alpha_2 \cap (\beta_1 \cup \beta_2)| = p + 1$

(ii) $\beta_1(1) = \alpha_2(|q|)$

(iii) $< \alpha_2, \beta_1 > (\beta_1(1)) = \text{sign}(q)$.

In other words, any two 2-bridge representations satisfying the above hypotheses are equal as knot diagrams. Furthermore, for such 2*-bridge representation, for any* $j = 1, 2$ *and* $n = 0, 1, \ldots, p$ *we have* $\beta_j(n) = \alpha_i[l]$ *where* $i \equiv n - j \mod 2$ *with* $i = 1, 2$ *and* $l \equiv nq \mod 2p$ *with* $0 \leq l < 2p$.

Proof. The hypothesis (i) gives us $p + 1$ intersection points on any α- and β-arcs by Lemma 3.2. First, we'll understand the structure of β_1. By Lemma 3.5, if we have $\beta_j(n) = \alpha_i[l]$, then $i \equiv n - j \mod 2$ with $i = 1, 2$. Then β_1 intersects with α_1 at the even-labelled points on α_1 and α_2 at the odd-labelled points on α_2. Without loss of generality assume $\text{sign}(q) = 1$, then our hypotheses give us $\beta_1(1) = \alpha_2[q]$ and the picture as in the Figure 3.6.

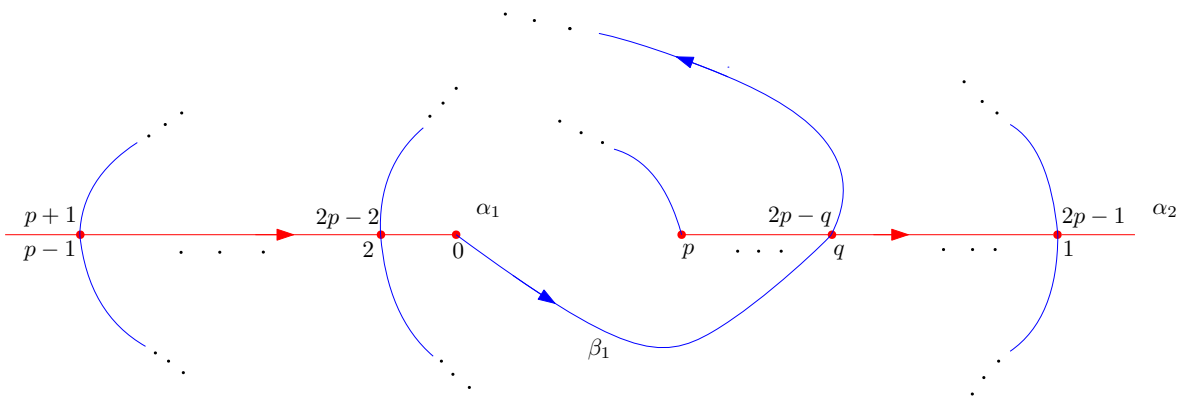

Figure 3.6. β_1 with its initial conditions.

Now, blow up α-arcs so that double labels on them split off and we get two circles as in the Figure 3.7. Then it is apparent that consecutive arcs must connect consecutive points. Initially, the point $\alpha_1[0]$ is connected to $\alpha_2[q]$ by β_1. In Figure 3.7, we see that the point $\alpha_1[2]$ must be connected to $\alpha_2[q-2]$ and the point $\alpha_1[2p-2]$ must be connected to $\alpha_2[q+2]$ by β_1.

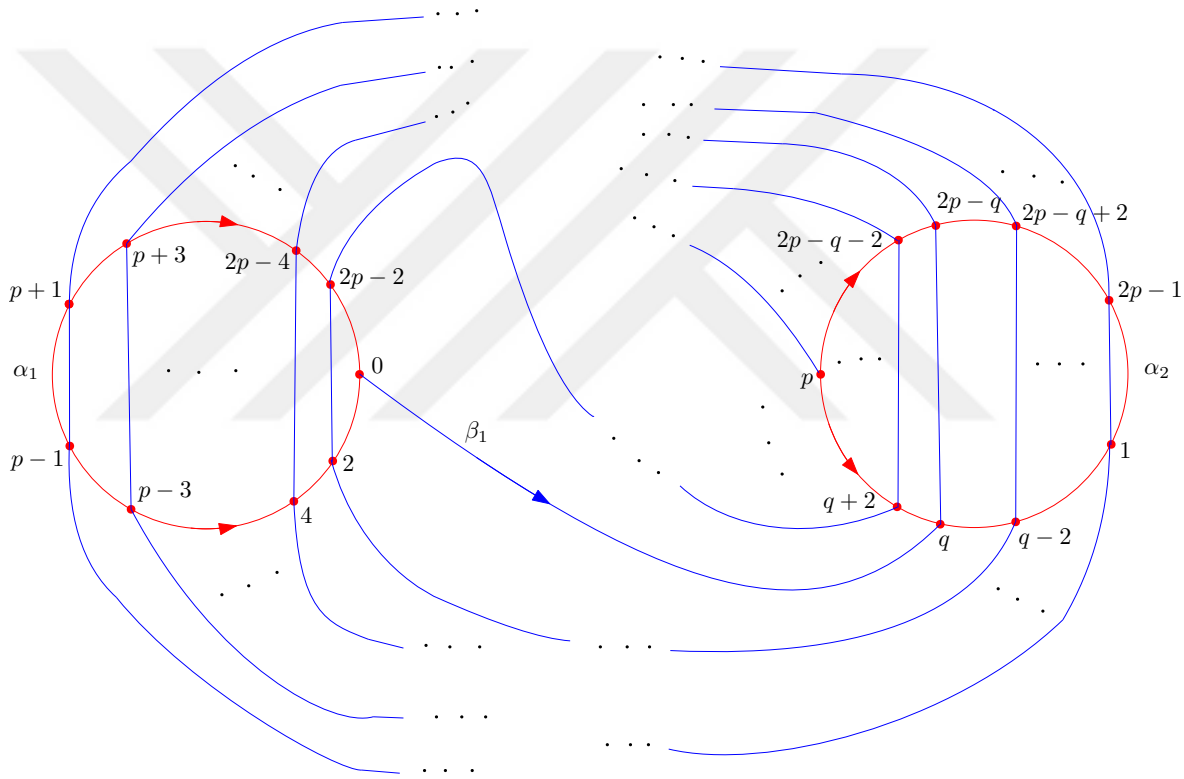

Figure 3.7. β_1 when α-arcs considered as circles.

Since consecutive arcs connects consecutive points, it is easy to see that if $\alpha_1[a]$ is connected to $\alpha_2[b]$, then we have $a+b \equiv q \mod 2p$. Without loss of generality assume β_1 goes from $\alpha_1[a]$ to $\alpha_2[b]$. Then $\beta_1(n) = \alpha_1[2p-a]$ and $\beta_1(n+1) = \alpha_2[b]$ for some n. Observe that $b-(2p-a) \equiv b+a-2p \equiv b+a \equiv q \mod 2p$. Hence, if $\beta_1(n) = \alpha_{i_1}[l_1]$ and $\beta_1(n+1) = \alpha_{i_2}[l_2]$, we get $l_2 - l_1 \equiv q \mod 2p$. Initially, we have $\beta_1(1) = \alpha_2(q)$, so by induction, $\beta_1(n) = \alpha_i[l]$ where $l \equiv nq \mod 2p$ with $0 \leq l < 2p$ for any n. Observe that the condition $\gcd(p,q) = 1$ guarantees that $\beta_1(n) = \beta_1(n')$ if $n \neq n'$.

Next, we need to understand the structure of β_2. But it is completely determined by the behaviour of β_1. The arc β_1 connects even-labelled points on α_1 with odd-labelled points on α_2, whereas β_2 connects odd-labelled points on α_1 with even-labelled points on α_2. Hence, between any consecutive arcs of β_1, there is an arc of β_2 that connects an odd-labelled points on α_1 with an even-labelled points on α_2. As an example, see Figure 3.8.

Obviously, we have $\beta_2(1) = \alpha_1(q)$ and if $\beta_2(n) = \alpha_{i_1}[l_1]$ and $\beta_2(n+1) = \alpha_{i_2}[l_2]$, we get $l_2 - l_1 \equiv q \mod 2p$. So by induction, $\beta_2(n) = \alpha_i[l]$ where $l \equiv nq \mod 2p$ with $0 \leq l < 2p$ for any n.

So, for any j and n, there is a unique i and l such that $\beta_j(n) = \alpha_i[l]$. This implies by Lemma 3.6 that there is a unique 2-bridge representation satisfying hypotheses (i), (ii) and (iii). $\square$

Now, for any odd integers p, q with $p \geq 3$, $-p < q < p$ and $\gcd(p,q) = 1$, we can define the *Schubert normal form* $S(p,q)$ as the 2-bridge representation (or as the knot that it represents) that satisfies the hypotheses of Theorem 3.7. By convention, we orient α_2 in the direction of negative u-axis as opposed to the property (ii) of bridge diagrams. For an example, see Figure 3.9. Also, it is obvious to see that the mirror image of $S(p,q)$ is $S(p,-q)$.

Corollary 3.8. *Any 2-bridge knot k is equivalent to $S(p,q)$ for some odd integers p, q with $p \geq 3$, $-p < q < p$ and $\gcd(p,q) = 1$.*

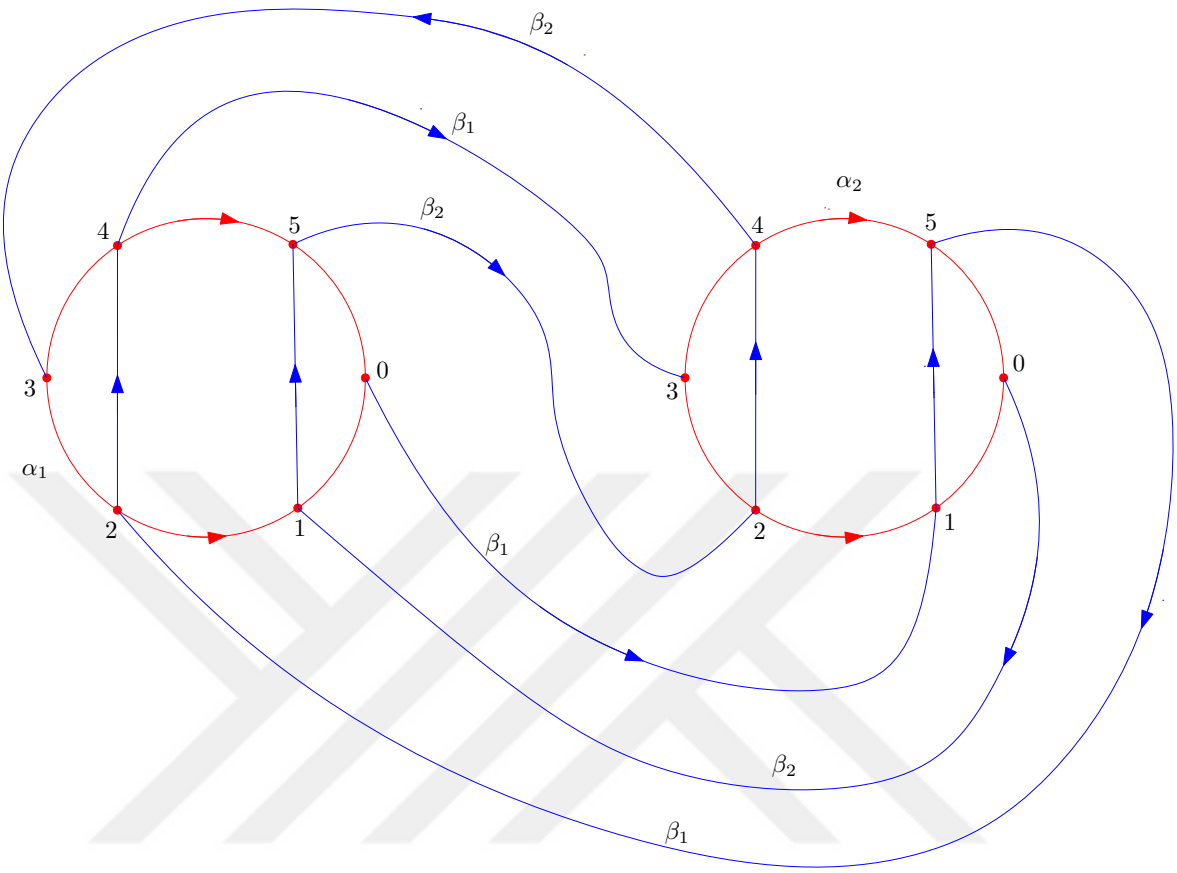

Figure 3.8. The 2-bridge knot with $p = 3$ and $q = 1$ (α-arcs considered as circles).

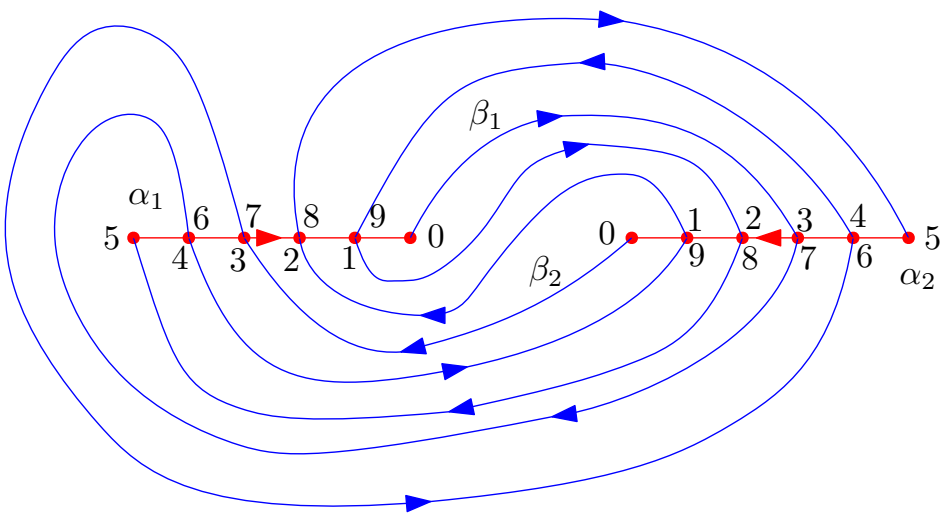

Figure 3.9. $S(5, 3)$ (The figure-eight knot).

Proof. By Corollary 2.5, k has a 2-bridge representation d. Lemma 3.2 implies that d satisfies the hypothesis (i) of Theorem 3.7 for some odd p and $p \geq 3$ and Lemma 3.3 implies that d satisfies the hypothesis (ii) of Theorem 3.7 for some odd q. Also obviously, $-p < q < p$. The hypothesis (iii) of Theorem 3.7 is also satisfied by d for some q. Finally, we know from the proof of Theorem 3.7 that these conditions are enough to get the relation $\beta_1(n) = \alpha_i[l]$ where $l \equiv nq \mod 2p$ with $0 \leq l < 2p$ for any n. If $\gcd(p, q) \neq 1$, we can find $n < p$ such that $\beta_1(n) = \alpha_i[p]$ which implies $\beta_1(n) = \beta_1(p)$ and hence $n = p$. But $n < p$, which gives a contradiction. Therefore, $\gcd(p, q) = 1$ and since all the hypotheses of Theorem 3.7 are satisfied by d, we see that d is equal to $S(p, q)$. □

3.2. Heegaard Diagrams

Our next aim is to understand which $S(p, q)$ are equivalent. But for this, we must exploit the interplay between knot theory and 3-manifold theory. In particular, we must understand the Heegaard decompositions and Heegaard diagrams of 3-manifolds. The most of the definitions and theorems given in this section is from [3].

A *genus g handlebody* U is a manifold diffeomorphic to a regular neighborhood of $\bigvee_{i=1}^{g} S^1$ in $\mathbb{R}^3$ (see Figure 3.10). Genus 0 handlebody is defined as D^3. The boundary of U is an oriented surface, called *genus g surface* Σ_g.

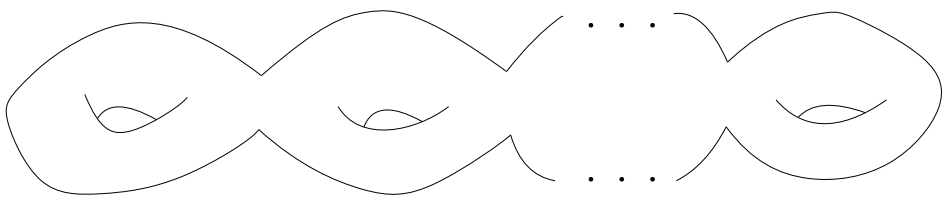

Figure 3.10. Genus g handlebody (with solid interior).

If U_0 and U_1 are genus g handlebodies, and if we glue them together along their common boundary, we get a closed 3-manifold $Y = U_0 \cup_{\Sigma_g} U_1$ which is oriented so that Σ_g is the oriented boundary of U_0. This is called a *genus g Heegaard decomposition*

for Y and it is usually referred as (Σ_g, U_0, U_1). Figure 3.11 shows a genus 0 Heegaard decomposition of S^3.

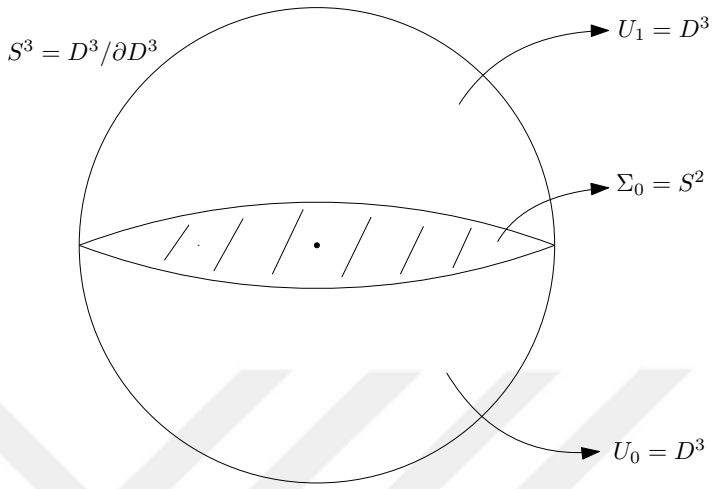

Figure 3.11. Genus 0 Heegaard decomposition of S^3 (considered as $D^3/\partial D^3$).

For any given Heegaard decomposion (Σ_g, U_0, U_1) of a closed, oriented 3-manifold Y, we can define another decomposition of genus $g+1$, by choosing two points in Σ_g and connecting them by an unknotted arc γ in U_1. Let N be a small tubular neighborhood of γ. Define $U_0' := U_0 \cup N$ and $U_1' = U_1 \setminus N$. Then obviously, $\partial U_0' = \partial U_1' = \Sigma_{g+1}$ and $Y = U_0' \cup_{\Sigma_{g+1}} U_1'$. We call $(\Sigma_{g+1}, U_0', U_1')$ as the *stabilization* of (Σ_g, U_0, U_1). See Figure 3.12 for a genus 1 Heegaard decomposition of S^3, which is the stabilization of the Heegaard decomposition shown in Figure 3.11.

We can glue handlebodies to get closed, oriented 3-manifolds. In fact, the converse is true also:

Theorem 3.9. *Let Y be a closed, oriented 3-manifold. Then Y admits a Heegaard decomposition.*

Proof. By Moise's theorem [4], every 3-manifold has a triangulation. The union of the vertices and edges of this triangulation gives a graph in Y. Let U_0 be a small regular neighborhood of this graph. Y is closed and oriented, hence U_0 is a handlebody. Also, $Y \setminus \operatorname{Int} U_0$ is a handlebody with same genus, since it is given by a regular neighborhood

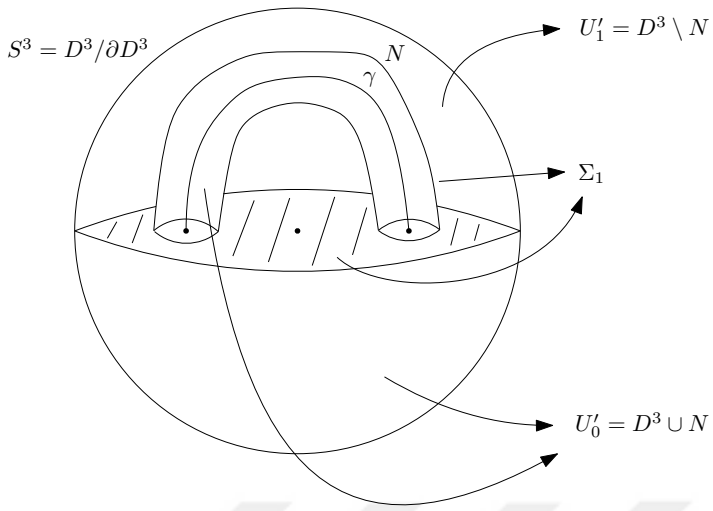

Figure 3.12. Genus 1 Heegaard decomposition of S^3 (considered as $D^3/\partial D^3$).

of the graph with the vertices as the centers of triangles and tetrahedrons and the edges connecting them. □

We know also that all Heegaard decompositions look the same after some stabilizations:

Theorem 3.10. *Let (Σ_g, U_0, U_1) and $(\Sigma'_{g'}, U'_0, U'_1)$ be two Heegaard decompositions of a closed, oriented 3-manifold Y. Then there exist n such that if we stabilize the first decomposition $n-g$ times and the second $n-g'$ times, we get two diffeomorphic Heegaard decompositions.*

Proof. See Singer [5]. □

A *set of attaching circles* $\gamma = (\gamma_1, \gamma_2, \ldots, \gamma_g)$ for a genus g handlebody U is a collection of closed embedded curves in $\Sigma_g = \partial U$ with the following properties:

(i) The curves γ_i are disjoint from each other.
(ii) $\Sigma_g \setminus (\gamma_1 \cup \gamma_2 \cup \ldots \gamma_g)$ is connected.
(iii) The curves γ_i bound disjoint embedded disks in U.

Note that we can restate the property (ii) as the property that $[\gamma_1], [\gamma_2], \ldots, [\gamma_g]$ are linearly independent $H_1(\Sigma_g, \mathbb{Z})$. Also note that the attaching circles correspond to the meridians of the handlebody U.

For a Heegaard decomposition (Σ_g, U_0, U_1) of Y, a compatible *Heegaard diagram* is given by Σ_g together with a collection of curves $\alpha = (\alpha_1, \alpha_2, \ldots, \alpha_g)$ and $\beta = (\beta_1, \beta_2, \ldots, \beta_g)$ such that α is a set of attaching circles for U_0 and β is a set of attaching circles for U_1. Such a Heegaard diagram is represented as $(\Sigma_g, \alpha, \beta)$. For an example, see Figure 3.13, which is a compatible Heegaard diagram of the Heegaard decomposition in Figure 3.12. It is obvious that α_1 and β_1 are closed embedded curves in Σ_1 that satisfy the properties (i), (ii) and (iii) of the set of attaching circles.

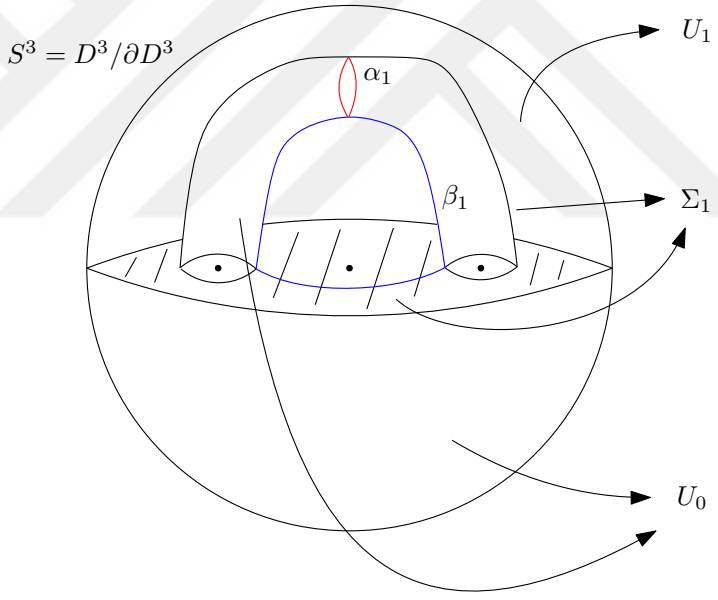

Figure 3.13. A Heegaard diagram $(\Sigma_1, \alpha_1, \beta_1)$ of S^3.

Conversely, any diagram $(\Sigma_g, \alpha, \beta)$ where α and β curves satisfy the properties (i) and (ii) of the set of attaching circles determine a unique Heegaard decomposition and hence a unique closed, oriented 3-manifold. For an example, see Figure 3.14. There, α_1 and β_1 are closed embedded curves in Σ_1 that satisfy the properties (i) and (ii) of the set of attaching circles, hence $(\Sigma_1, \alpha_1, \beta_1)$ determines a unique closed, oriented 3-manifold, which is $S^1 \times S^2$. We could choose $\beta_1 = \alpha_1$, then we get $S^1 \times S^2 = (\Sigma_1, \alpha_1, \alpha_1)$.

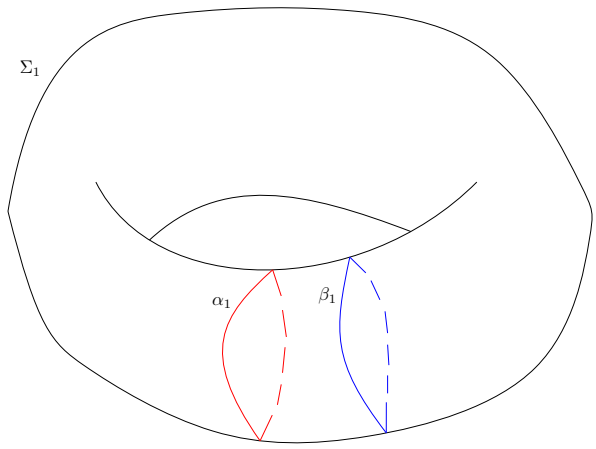

Figure 3.14. A Heegaard diagram $(\Sigma_1, \alpha_1, \beta_1)$ of $S^1 \times S^2$.

Now, we will define three operations on Heegaard diagrams, called *Heegaard moves*. The first two operations can be described for attaching circles $\gamma_1, \gamma_2, \ldots, \gamma_g$ for a given handlebody U. An *isotopy* moves $\gamma_1, \gamma_2, \ldots, \gamma_g$ in one parameter family so that the curves remain disjoint during isotopy. A *handle slide* of γ_1 over γ_2 is the process during which we replace γ_1 with γ_1' provided that γ_1' is a simple closed curve which is disjoint from $\gamma_1, \gamma_2, \ldots, \gamma_g$ with the property that γ_1', γ_1 and γ_2 bound an embedded pair of pants in $\Sigma_g \setminus (\gamma_3 \cup \cdots \cup \gamma_g)$. We have the following theorem regarding these two operations:

Theorem 3.11. *Let $(\gamma_1, \gamma_2, \ldots, \gamma_g)$ and $(\gamma_1', \gamma_2', \ldots, \gamma_g')$ be two sets of attaching circles for a handlebody U. Then these two sets can be connected by a sequence of isotopies and handle slides.*

Proof. See Scharlemann and Thompson [6]. □

The last operation on Heegaard diagrams is defined as follows: For a Heegaard diagram $(\Sigma_g, \alpha, \beta)$ with $\alpha = (\alpha_1, \alpha_2, \ldots, \alpha_g)$ and $\beta = (\beta_1, \beta_2, \ldots, \beta_g)$, define Σ_{g+1}' as the connected sum of Σ_g with Σ_1 and replace α and β by $\alpha' = (\alpha_1, \alpha_2, \ldots, \alpha_{g+1})$ and $\beta' = (\beta_1, \beta_2, \ldots, \beta_{g+1})$ respectively, where α_{g+1} and β_{g+1} are simple closed curves that are supported in Σ_1 which intersect at a single point transversally. Then, $(\Sigma_{g+1}', \alpha', \beta')$ is

called the *stabilization* of $(\Sigma_g, \alpha, \beta)$. Note that in this case, the Heegaard decomposition given by $(\Sigma'_{g+1}, \alpha', \beta')$ is the stabilization of the Heegaard decomposition given by $(\Sigma_g, \alpha, \beta)$. Then we have the following theorem:

Theorem 3.12. *Let $(\Sigma_g, \alpha, \beta)$ and $(\Sigma'_{g'}, \alpha', \beta')$ be two Heegaard diagrams of a closed, oriented 3-manifold Y. Then, they are diffeomorphic after applying a sequence of Heegaard moves to each of them.*

Proof. The Heegaard diagrams $(\Sigma_g, \alpha, \beta)$ and $(\Sigma'_{g'}, \alpha', \beta')$ give two Heegaard decompositions (Σ_g, U_0, U_1) and $(\Sigma'_{g'}, U'_0, U'_1)$. By Theorem 3.10 after stabilizations we get (Σ_n, V_0, V_1) and (Σ'_n, V'_0, V'_1) respectively, which are diffeomorphic. Then for each handlebody, attaching circles can be connected by a sequence of isotopies and handle slides by Theorem 3.11. Hence, we get two diffeomorphic Heegaard diagrams. □

We can also define the *pointed Heegaard diagram* as $(\Sigma_g, \alpha, \beta, z)$ where $(\Sigma_g, \alpha, \beta)$ is a Heegaard diagram and $z \in \Sigma_g \setminus (\alpha_1 \cup \ldots \alpha_g \cup \beta_1 \cup \cdots \cup \beta_g)$ is a point, called the *basepoint*. For pointed Heegaard diagrams, we can define the *pointed Heegaard moves*: A *pointed isotopy* moves $\gamma_1, \gamma_2, \ldots, \gamma_g$ and z in one parameter family so that the curves and the point z remain disjoint during isotopy. A *pointed handle slide* of γ_1 over γ_2 is the process during which we replace γ_1 with γ'_1 provided that γ'_1 is a simple closed curve which is disjoint from $\gamma_1, \gamma_2, \ldots, \gamma_g$ and z with the property that γ'_1, γ_1 and γ_2 bound an embedded pair of pants in $\Sigma_g \setminus (\gamma_3 \cup \cdots \cup \gamma_g \cup z)$. A *pointed stabilization* is the same as the usual stabilization. We have the pointed version of the Theorem 3.11 and 3.12:

Theorem 3.13. *Let $(\gamma_1, \gamma_2, \ldots, \gamma_g)$ with the basepoint z and $(\gamma'_1, \gamma'_2, \ldots, \gamma'_g)$ with the basepoint z' be two sets of attaching circles for a handlebody U. Then these two sets and their basepoints can be connected by a sequence of pointed isotopies and pointed handle slides.*

Theorem 3.14. *Let $(\Sigma_g, \alpha, \beta, z)$ and $(\Sigma'_{g'}, \alpha', \beta', z')$ be two pointed Heegaard diagrams of a closed, oriented 3-manifold Y. Then, they are diffeomorphic after applying a sequence of pointed Heegaard moves to each of them.*

There is a useful way to represent the Heegaard diagram $(\Sigma_g, \alpha, \beta)$: We consider the plane $\mathbb{R}^2$ (with the point at infinity) as S^2 and remove interiors of g pairs of disks from C. For each pair, we identify the boundaries of disks (circles) so that under identification, we see two circles as mirror images of each other. Obviously, under such identification, our plane becomes Σ_g. Then we draw α and β curves on that plane. See Figure 3.15 for an example.

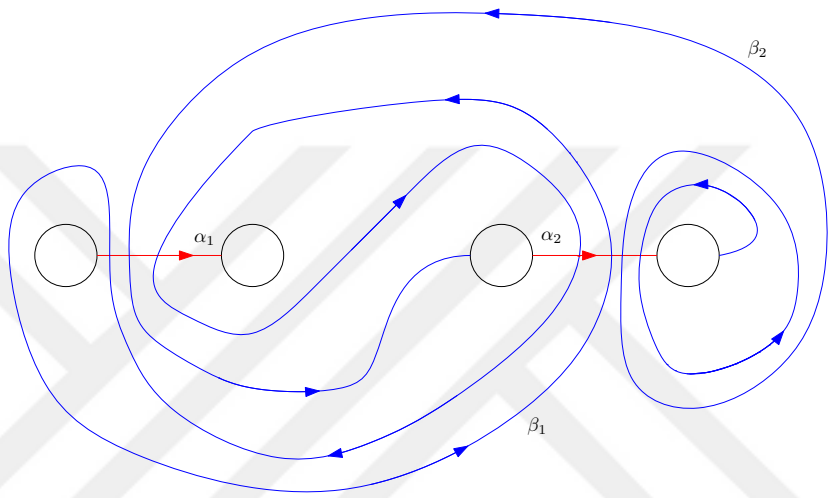

Figure 3.15. A genus 2 Heegaard diagram.

Furthermore, we can talk about the homology classes of attaching circles. Fix an orientation on each attaching circle. Homology class of each attaching circle is an element of $H_1(\Sigma_g, \mathbb{Z})$, which is generated by meridians and longitudes (see Figure 3.16). In particular, for $g = 1$, the homology classes completely determine the attaching circles.

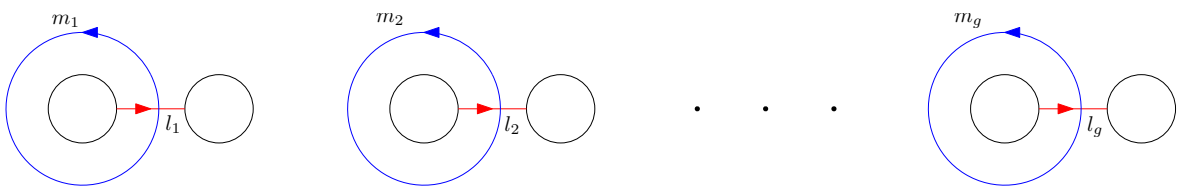

Figure 3.16. Meridians and longitudes of Σ_g.

Observe that $< l_i, m_i >= 1$ (and therefore $< m_i, l_i >= -1$) for all i and all the other algebraic intersections are zero. If γ is an attaching circle, then $[\gamma] = a_1[m_1] +$

$b_1[l_1] + \cdots + a_g[m_g] + b_g[l_g]$. Hence,

$$\begin{aligned} < l_i, \gamma > &= a_1 < l_i, m_1 > + b_1 < l_i, l_1 > + \cdots + a_g < l_i, m_g > + b_g < l_i, l_g > \\ &= a_i \end{aligned}$$

Also we have,

$$\begin{aligned} < m_i, \gamma > &= a_1 < l_i, m_1 > + b_1 < m_i, l_1 > + \cdots + a_g < m_i, m_g > + b_g < m_i, l_g > \\ &= -b_i \end{aligned}$$

So, we can determine the homology class of γ by calculating $a_i =< l_i, \gamma >$ and $b_i = - < m_i, \gamma >$ for all i.

For example, with this method, we can express the Heegaard diagram in Figure 3.15 without drawing any actual diagram. Orient α and β curves as shown in the figure. Obviously, we have $[\alpha_1] = [l_1]$ and $[\alpha_2] = [l_2]$. For β_1, we have $< l_1, \beta_1 >= -1$, $< m_1, \beta_1 >= 0$, $< l_2, \beta_1 >= 0$ and $< m_2, \beta_1 >= 0$, hence $[\beta_1] = -[m_1]$. For β_2, we have $< l_1, \beta_2 >= -1$, $< m_1, \beta_2 >= 0$, $< l_2, \beta_2 >= -2$ and $< m_2, \beta_2 >= 1$, hence $[\beta_2] = -[m_1] - 2[m_2] - [l_2]$. So, the Heegaard diagram is $(\Sigma_2, \alpha, \beta)$ where $[\alpha_1] = [l_1]$, $[\alpha_2] = [l_2]$, $[\beta_1] = -[m_1]$ and $[\beta_2] = -[m_1] - 2[m_2] - [l_2]$.

For any integers p, q such that $p > 0$, $-p < q < p$, $\gcd(p, q) = 1$ and q odd, we can define the *Lens space* $L(p, q)$ as the closed, orientable 3-manifold given by the Heegaard diagram $(\Sigma_1, \alpha_1, \beta_1)$ where $[\alpha_1] = [m_1]$ and $[\beta_1] = q[m_1] + p[l_1]$. We will see that there is a strong connection between Lens spaces and 2-bridge knots. We close up this section with the classification theorem of Lens spaces:

Theorem 3.15. *The Lens spaces $L(p, q)$ and $L(p', q')$ are homeomorphic if and only if $p = p'$ and $q^{\pm 1} \equiv q' \mod p$, where q^{-1} denotes the integer with the properties $0 < q^{-1} < 2p$ and $qq^{-1} \equiv 1 \mod 2p$.*

Proof. See Reidemeister [7] and Brody [8]. □

3.3. Branched Coverings

We'll analyse the double branched coverings of S^3 branched along 2-bridge knots, which will be the connection between knots and 3-manifold and our main tool when dealing with the classification of 2-bridge knots. In this section, we will define branched coverings and deal with some useful examples.

First, consider the following map which will be the prototype for branched coverings:

$$\begin{aligned} h : \mathbb{C} &\longrightarrow \mathbb{C} \\ z &\longmapsto z^n \end{aligned}$$

for some fixed $n \in \mathbb{N}$ and $n \geq 2$. Note that for each $w \in \mathbb{C} \setminus \{0\}$, $|h^{-1}(w)| = n$, but $|h^{-1}(0)| = 1$. We say that h is the n-fold branched covering of $\mathbb{C}$ (the codomain), branched along the point 0. We also say that $\mathbb{C}$ (the domain) is the n-fold branched covering of $\mathbb{C}$ (the codomain), branched along the point 0.

More generally, for two manifolds M and N with the same dimension and a nowhere dense subset B of N with the codimension 2, we say that the function $f : M \to N$ is the *n-fold branched covering of N branched along B* (called *branch set*) if f is an n-fold covering of N except for the set B and around each point $w \in B$, f looks like the map h above (in some coordinate chart) where $w \in B$ corresponds to $0 \in \mathbb{C}$. Again, in this case we usually say that M is the n-fold branched covering of N branched along B.

Now, we'll consider some double branched coverings. Consider the space D^2. Let τ be the rotation by the angle π around the axis that passes through the origin of D^2. Then the quotient map $\pi : D^2 \to D^2/\tau$ is the double branched covering of $D^2/\tau \cong D^2$ branched along the origin, see Figure 3.17. Note that D^2/τ means $D^2/(x \sim \tau(x))$ actually. Also, note that the arcs a are identified as shown with arrows in the figure.

In this case, we say that D^2 is the double branched covering of D^2 branched along one point.

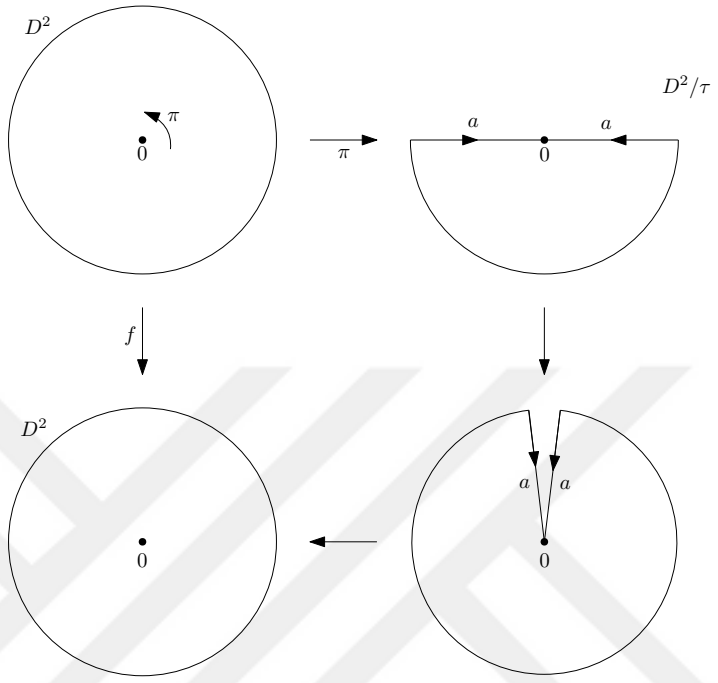

Figure 3.17. The double branched covering of D^2 branched along one point.

Next, consider the genus g surface Σ_g. Let τ be the rotation by the angle π around the axis that passes through the points $P_1, P_2, \ldots, P_{2g+2}$ of Σ_g as shown in Figure 3.18. Then the quotient map $\pi : \Sigma_g \to \Sigma_g/\tau$ is the double branched covering of $\Sigma_g/\tau \cong S^2$ branched along the points $P_1, P_2, \ldots, P_{2g+2}$, see Figure 3.18. Note that the arcs a_i are identified as shown with arrows in the figure. In this case, we say that Σ_g is the double branched covering of S^2 branched along $2g+2$ points.

Finally, we will consider a genus g handlebody U. Let τ be the rotation by the angle π around the axis that passes through the arcs $l_1, l_2, \ldots, l_{g+1}$ in U as shown in Figure 3.19. Then the quotient map $\pi : U \to U/\tau$ is the double branched covering of $U/\tau \cong D^3$ branched along the arcs $l_1, l_2, \ldots, l_{g+1}$, see Figure 3.19. Note that the areas a_i are identified as shown with arrows in the figure. In this case, we say that genus g handlebody U is the double branched covering of D^3 branched along $g+1$ arcs.

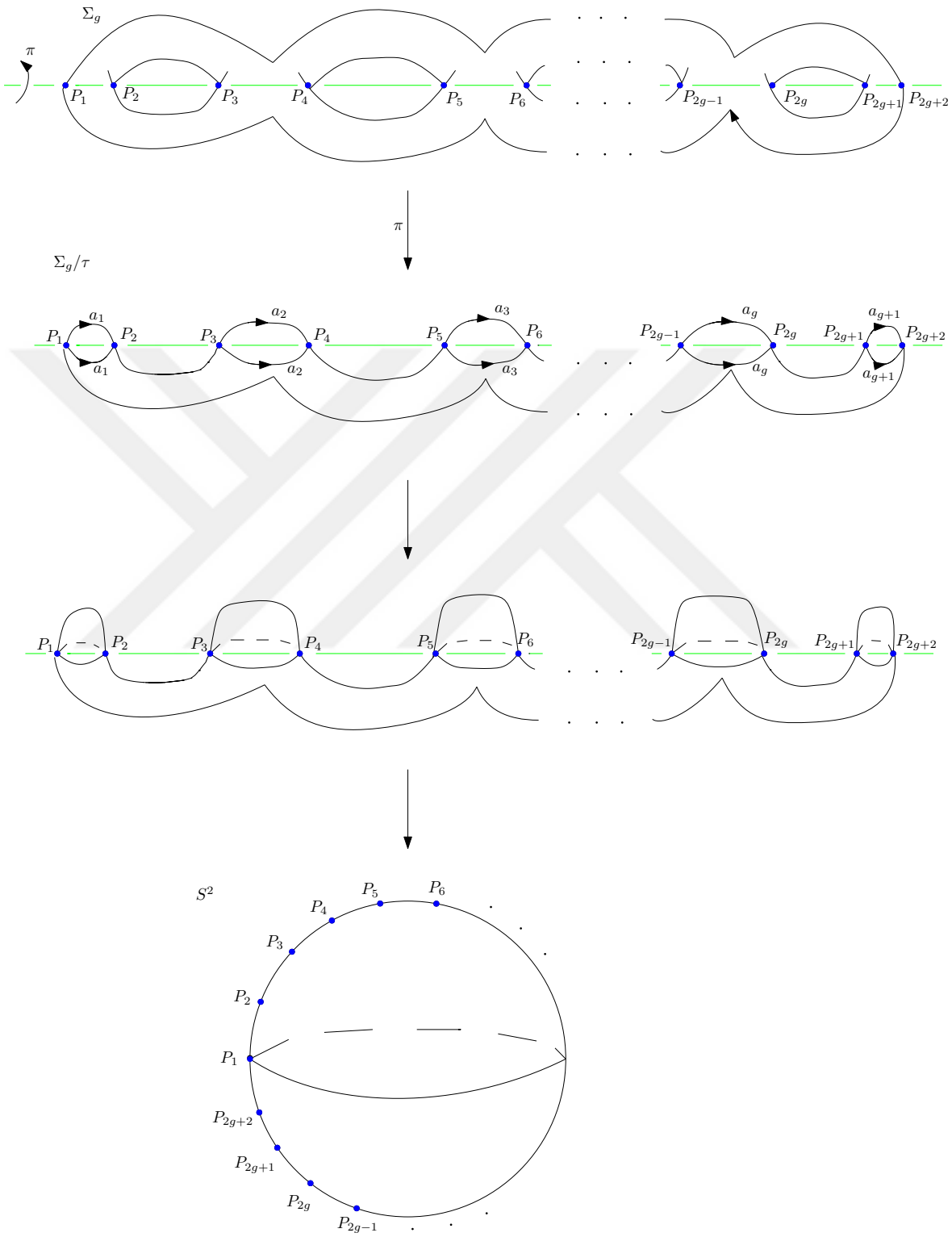

Figure 3.18. The double branched covering of S^2 branched along $2g+2$ points.

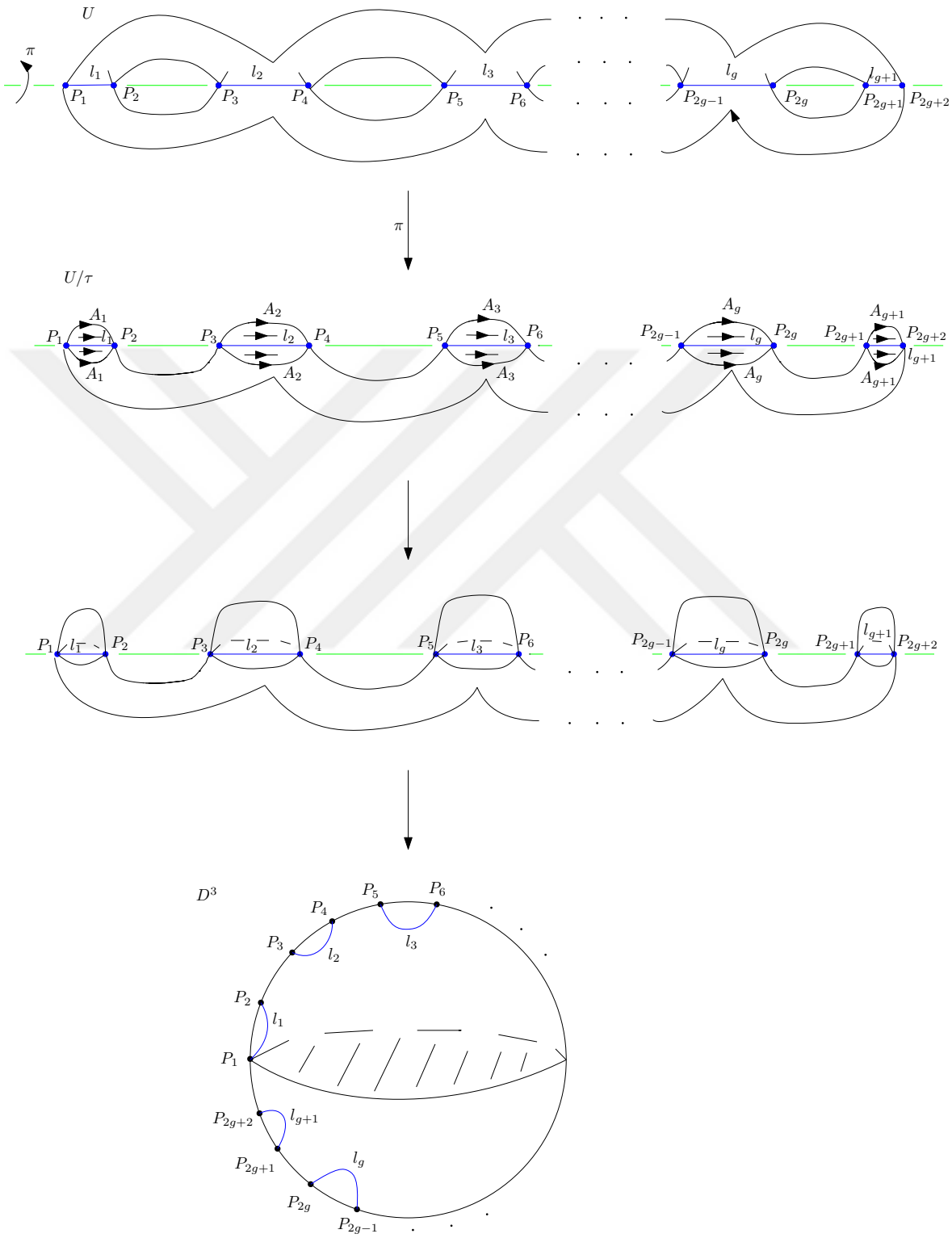

Figure 3.19. The double branched covering of D^3 branched along $g+1$ arcs.

3.4. Classification of 2-Bridge Knots

By Corollary 3.8, we know that any 2-bridge knot can be represented as $S(p,q)$. Now, we want to find the necessary and sufficient condition on p, q, p', q' which gives $S(p,q) = S(p',q')$. This will provide us the classification of 2-bridge knots. We will find this condition using the techniques we developed.

We can consider knots as if they lie in S^3. Our aim is to determine the double branched covering of S^3 branched along $S(p,q)$.

Theorem 3.16. *The double branched covering of S^3 branched along $S(p,q)$ is the Lens space $L(p,q)$.*

Proof. Consider S^3 as $D^3/\partial D^3$ and project knots into its equator, which is $D^2/\partial D^2 = S^2$. Start with the 2-bridge representation of $S(p,q)$ on S^2 (i.e. $E = S^2$). We know that this representation has two underbridges α_1, α_2 and two overbridges β_1, β_2. To get the original knot in S^3 from its representation on S^2, we can push α-arcs down (i.e in $-u \times v$ direction) and β-arcs up (i.e in $u \times v$ direction). See Figure 3.20.

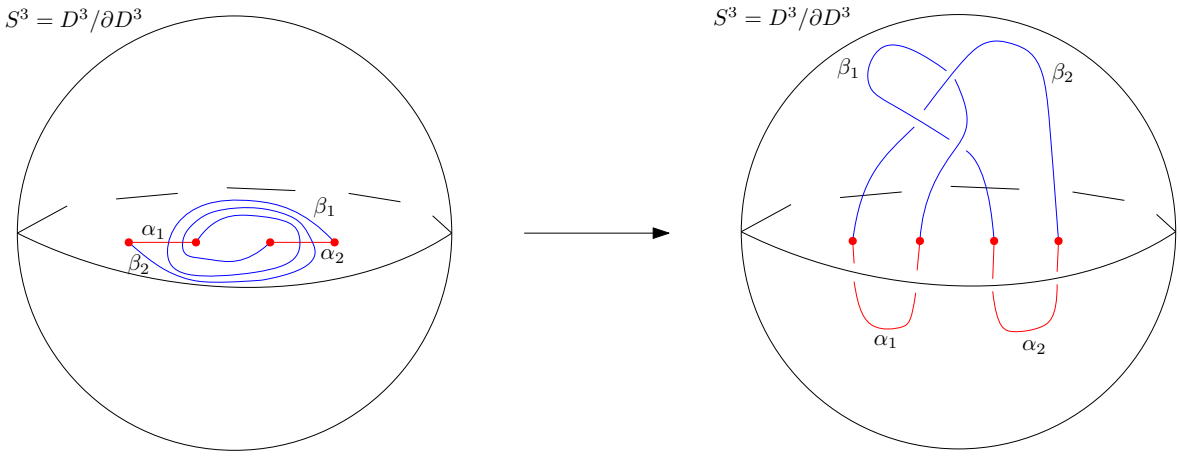

Figure 3.20. $S(3,1)$ in S^3.

We call the lower part of S^3 with the equator as B_0 and the upper part of S^3 with the equator as B_1. Then obviously, $B_i = D^3$ for any $i = 1, 2$ and $S^3 = B_0 \cup_{S^2} B_1$

where S^2 is the equator. Also, α-arcs lie in B_0, β-arcs lie in B_1 and the endpoints $\alpha(0), \alpha(p), \beta(0), \beta(p)$ lie in the equator S^2.

We want to find the double branched covering of $S^3 = B_0 \cup_{S^2} B_1$ branched along $S(p,q)$. So, we need to find the double branched covering of

(i) B_0 along α-arcs.
(ii) B_1 along β-arcs.
(iii) S^2 along four endpoints $\alpha_0, \alpha_p, \beta_0, \beta_p$.

In Section 3.3, we have showed that the double branched covering of D^3 branched along $g+1$ arcs is the genus g handlebody. Since we have two arcs for each B_i, the double branched covering of B_0 branched along α-arcs is the genus 1 handlebody U_0. Similarly, the double branched covering of B_1 branched along β-arcs is the genus 1 handlebody U_1. Again in Section 3.3, we have showed that the double branched covering of S^2 branched along $2g+2$ points is the genus g surface Σ_g. Hence, the double branched covering of S^2 branched along four endpoints $\alpha_0, \alpha_p, \beta_0, \beta_p$ is genus 1 surface Σ_1.

These results imply that the double branched covering of $S^3 = B_0 \cup_{S^2} B_1$ branched along $S(p,q)$ is $U_0 \cup_{\Sigma_1} U_1$. We know from Section 3.2 that this is a Heegaard decomposition of a closed, oriented 3-manifold. To understand this manifold, we need to explain the gluing map that connects U_0 and U_1 along the surface Σ_1.

From Section 3.2, we know that it is enough to show to describe how the attaching circles (i.e. meridians) of U_0 and U_1 look like on the boundary Σ_1. Also we know from Section 3.2 that for $g = 1$ the attaching circles are completely determined by their homology classes. Hence, our aim is to define the homology classes of the meridians of U_0 and U_1, in terms of the homology classes of meridian m_1 and longitude l_1 of Σ_1.

Let us call the attaching circle of U_0 as a_1 and the attaching circle of U_1 as b_1. If we see Σ_1 as the boundary of U_0 and U_1 as the handlebody attached to Σ_1, we get $a_1 = m_1$. So, only thing we need to describe is $[b_1]$. Our strategy will be the following:

First, we'll describe m_1 and l_1 using α_1 and γ_1. Then, we will describe b_1 using β_1. We know all the knowledge about the intersections between α_1 and β_1, so using this, we will pass to describing $[b_1]$ using $[m_1]$ and $[l_1]$.

First, we claim that a_1 is the lift of α_1 on S^2 to the branched covering Σ_1. Also, the lift of α_2 gives us another (equivalent) meridian, call it a_2. This can be observed from Figure 3.18 and it is shown explicitly in Figure 3.21.

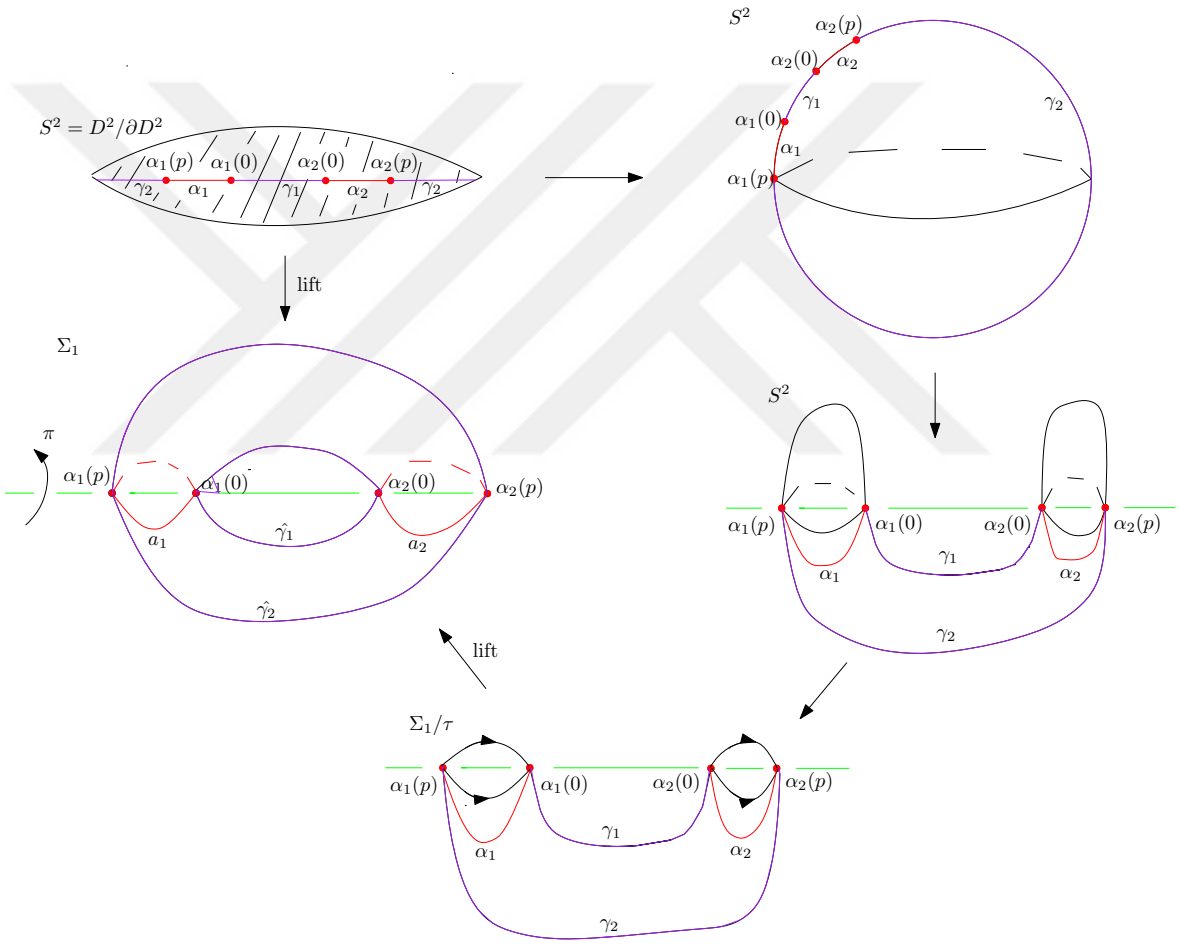

Figure 3.21. The lifts of the arcs $\alpha_1, \alpha_2, \gamma_1, \gamma_2$.

Denote the lift of any set s to the branched covering as $\hat{s}$. Then we have $a_1 = \hat{\alpha_1}$ and $a_2 = \hat{\alpha_2}$. Similarly, we have $b_1 = \hat{\beta_1}$ and $b_2 = \hat{\beta_2}$ where b_2 is the another meridian (equivalent to b_1) for U_1.

Now, we have $[b_1] = c_1[m_1] + d_1[l_1]$ and want to find c_1 and d_1. From Sec-

tion 3.2, we know $c_1 =< l_1, b_1 >$ and $d_1 = - < m_1, b_1 >$. We have $m_1 = a_1$, so $d_1 = - < a_1, b_1 >= - < \hat{\alpha_1}, \hat{\beta_1} >$. We know that β_1 intersects with α_1 and α_2 alternately. Hence b_1 intersects with a_1 and a_2 alternately. Since a_1 and a_2 are meridians, $< a_1, b_1 > (z)$ are the same for any intersection point z. Orient a_1 and b_1 so that we have $< a_1, b_1 > (z) = -1$ for all intersection points z. Then we have

$$< a_1, b_1 >= -|a_1 \cap b_1| = -|\hat{\alpha_1} \cap \hat{\beta_1}|$$

Obviously, in $\alpha_1 \cap \beta_1$, there is no branch point except the common endpoint $\alpha_1(0) = \beta_1(0)$. Also, we know from Lemma 3.1 and 3.2 that $|\alpha_1 \cap \beta_1| = (p+1)/2 = (p-1)/2 + 1$. Then we have $|\hat{\alpha_1} \cap \hat{\beta_1}| = 2 * (p-1)/2 + 1 = p$. Hence $d_1 = |\hat{\alpha_1} \cap \hat{\beta_1}| = p$.

Next, we want to find $c_1 =< l_1, b_1 >$. For this, we need to describe l_1. We can show that $l_1 = \hat{\gamma_1}$ where γ_1 is an arc connecting $\alpha_1(0)$ and $\alpha_2(0)$. Also, $l_2 = \hat{\gamma_2}$ where γ_2 is an arc connecting $\alpha_1(p)$ and $\alpha_2(p)$ and l_2 is a longitude of Σ_1 (equivalent to l_1). See Figure 3.21.

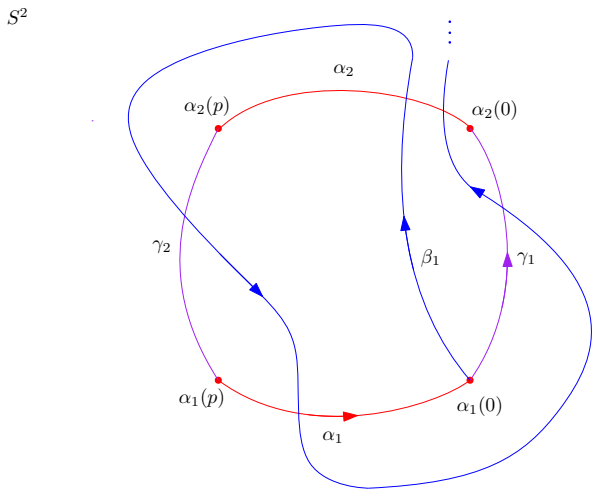

Figure 3.22. Intersections between β_1 and γ_1.

We orient l_1 so that we have $< l_1, m_1 >= 1$. From the Figure 3.22, we observe the followings:

(i) Apart from the endpoint $\alpha_1(0)$, β_1 first intersects with γ_2 and lastly intersects

with γ_1.

(ii) β_1 intersects with γ_1 and γ_2 alternately.

(iii) By isotopy, we can get a diagram in which β_1 intersects with γ_j after intersecting α_i at $\beta_1(n)$ if and only if there is a turning, i.e. $< \alpha_i, \beta_1 > (\beta_1(n)) \neq < \alpha_i, \beta_1 > (\beta_1(n+1))$.

By the observation (ii) above, we obviously see that b_1 intersects with l_1 and l_2 alternately. This gives us that $< l_1, b_1 > (z)$ is the same for every intersection point z. Since the orientations of l_1 and b_1 are fixed, we see from the Figure 3.22 that $< l_1, b_1 > (z) = \text{sign}(q)$ for each intersection points z. Hence we have

$$< l_1, b_1 >= \text{sign}(q)|l_1 \cap b_1| = \text{sign}(q)|\hat{\gamma_1} \cap \hat{\beta_1}|$$

The only branch point in $\gamma_1 \cap \beta_1$ are the common endpoint $\alpha_1(0)$. We also have even number of turnings from the observations (i) and (ii), hence half of them are consisting of the intersections between β_1 and γ_1 (except at $\alpha_1(0)$). But since they will be lifted and they are not branch points, we will count them twice. Hence $|\hat{\gamma_1} \cap \hat{\beta_1}|$ is equal to the number of turnings plus 1 (the intersection at $\alpha_1(0)$).

By Theorem 3.7, we know that $\beta_1(n) = \alpha_i[l]$ where $l \equiv nq \mod 2p$ with $0 \leq l < 2p$. This condition obviously tells us that the number of turnings is $(p|q|)/|q| - 1 = |q| - 1$. Hence, $|\hat{\gamma_1} \cap \hat{\beta_1}| = |q| - 1 + 1 = |q|$. Therefore, $c_1 =< l_1, b_1 >= \text{sign}(q)|q| = q$.

We got the Heegaard diagram (Σ_1, a_1, b_1) with $[a_1] = [m_1]$ and $[b_1] = q[m_1] + p[l_1]$. From Section 3.2, we know that this is the Heegaard diagram of the Lens space $L(p, q)$. Hence, the double branched covering of S^3 branched along $S(p, q)$ is $L(p, q)$.

□

Obviously, if two 2-bridge knots have different branched coverings, then they are not equivalent. Therefore, the classification of Lens spaces (Theorem 3.15) gives us

a necessary condition for the equivalence of 2-bridge knots. However, we also showed that the explicit correspondence between 2-bridge knots and the Lens spaces by giving the recipe of getting the double branched covering of S^3 branched along a 2-bridge knot in Theorem 3.16. By exploiting this, we can get also the sufficient condition for the equivalence of 2-bridge knots from the classification of Lens spaces. Hence, we get the following theorem:

Theorem 3.17. *The 2-bridge knots $S(p,q)$ and $S(p',q')$ are equivalent if and only if $p = p'$ and $q^{\pm 1} \equiv q' \mod p$, where q^{-1} denotes the integer with the properties $0 < q^{-1} < 2p$ and $qq^{-1} \equiv 1 \mod 2p$.*

4. CONCLUSION

Corollary 3.8 and Theorem 3.17 together give us the classification of 2-bridge knots. Furthermore, by Theorem 3.7 we know the complete structure of Schubert normal forms and this provides us very deep understanding of 2-bridge knots. For example, using the Schubert normal form of a 2-bridge knot, we can compute its knot Floer homology very easily, which gives us in turn many invariants such as Alexander polynomial and signature. These invariants help us to decide whether a given knot is a 2-bridge knot or not.

REFERENCES

1. Schubert, H., "Knoten mit zwei Brücken", *Math. Z.*, Vol. 65, pp. 133–170, 1956.

2. Burde, G. and H. Zieschang, *Knots*, Vol. 5 of *de Gruyter Studies in Mathematics*, Walter de Gruyter & Co., Berlin, second edn., 2003.

3. Ozsváth, P. and Z. Szabó, "An introduction to Heegaard Floer homology", *Floer homology, gauge theory, and low-dimensional topology*, Vol. 5 of *Clay Math. Proc.*, pp. 3–27, Amer. Math. Soc., Providence, RI, 2006.

4. Moise, E. E., "Affine structures in 3-manifolds. V. The triangulation theorem and Hauptvermutung", *Ann. of Math. (2)*, Vol. 56, pp. 96–114, 1952.

5. Singer, J., "Three-dimensional manifolds and their Heegaard diagrams", *Trans. Amer. Math. Soc.*, Vol. 35, No. 1, pp. 88–111, 1933, `http://dx.doi.org/10.2307/1989314`.

6. Scharlemann, M. and A. Thompson, "Heegaard splittings of (surface) $\times$ I are standard", *Math. Ann.*, Vol. 295, No. 3, pp. 549–564, 1993, `http://dx.doi.org/10.1007/BF01444902`.

7. Reidemeister, K., "Homotopieringe und Linsenräume", *Abh. Math. Sem. Univ. Hamburg*, Vol. 11, No. 1, pp. 102–109, 1935, `http://dx.doi.org/10.1007/BF02940717`.

8. Brody, E. J., "The topological classification of the lens spaces", *Ann. of Math. (2)*, Vol. 71, pp. 163–184, 1960.